Structural and Multidisciplinary Optimization
https://doi.org/10.1007/s00158-020-02647-8

INDUSTRIAL APPLICATION PAPER

Lightweight optimization of passenger car seat frame based on grey relational analysis and optimized coefficient of variation

Zhiying Shan[1] · Jiangqi Long[1] · Ping Yu[1] · Liang Shao[1] · Yaoqing Liao[1]

Received: 7 January 2020 / Revised: 23 March 2020 / Accepted: 4 June 2020

Abstract

At present, the safety performance and lightweight of passenger car seat has become more and more important. The multi-objective lightweight optimization of the passenger car seat frame is carried out in this study. The novelty of this study is that we propose a detailed optimization design method and a design process in lightweight optimization for passenger car seat. In more detail, firstly, according to the ratio of energy absorption to mass method, the lightweight design components are selected. Secondly, different seat safety tests are conducted to optimize the corresponding components by considering both continuous thickness variables and discrete material variables. Thirdly, the strain index, the displacement of key points, the material cost, and the total mass of the components which need to be optimized (opti-components) are considered objectives. After that, the grey relational analysis (GRA) is adopted to optimize the material thickness scheme of the lightweight design components. Besides, the optimized coefficient of variation (OCV) method is applied to evaluate the corresponding weighting values of the objectives. Meanwhile, the availability of the grey relational analysis and optimized coefficient of variation (GRA&OCV) is assessed through comparing advantages among the method of GRA&OCV, the grey relational analysis and coefficient of variation (GRA&CV), the technique for order preference by similarity to ideal solution and coefficient of variation (TOPSIS&CV), as well as the technique for order preference by similarity to ideal solution and optimized coefficient of variation (TOPSIS&OCV) in the multi-objective lightweight optimization of passenger car seat frame. As a result, the total material cost and mass of the passenger car seat frame are reduced by 17.00% and by 2.08 kg (12.46%), respectively, with guaranteed vibrational and safety performance. Therefore, GRA&OCV can be effectively applied in multi-objective lightweight optimization of the passenger car seat frame.

Keywords Passenger car seat · Lightweight optimization · Grey relational analysis · Optimized coefficient of variation

Responsible Editor: Ren-Jye Yang

Electronic supplementary material The online version of this article (https://doi.org/10.1007/s00158-020-02647-8) contains supplementary material, which is available to authorized users.

✉ Jiangqi Long
longjiangqi@163.com

Zhiying Shan
zhiying_shan@163.com

Ping Yu
yuping55@wzu.edu.cn

Liang Shao
shaoliangtjauto@163.com

Yaoqing Liao
919615874@qq.com

[1] College of Mechanical and Electrical Engineering, Wenzhou University, Chashan street, Ouhai district, Wenzhou 325035, China

Nomenclature

A	the target value
A_i	the ith component area
a	the number of design variables
AOW	an optimization method performing global optimization by using alternative models, optimization algorithms and weight methods
APT	Antisubmarine Pan Test
B_i	the codes of components
C	the cost of material
CV	coefficient of variation
D_t	the standard deviation of the tth sequence
DOE	design of experiment
e	the number of inequality constraints
E_{Bi}	the post-fracture elongation of material of Bi component

Published online: 25 July 2020

E_i	the material elastic modulus
$E_{\partial_i - B_i}$	the energy absorption value of B_i component in ∂_i safety test
$f_\rho(M_i)$	the functional relation of the material type M_i and the density ρ_i
$f_E(M_i)$	the functional relation of the material type M_i and the material elastic modulus E_i
$f_P(M_i)$	the functional relation of the material type M_i and the material price P_i
FULT	Frame Ultimate Load Test
G	the total mass of passenger car seat frame
G_{Bi}	the mass of the *Bi* components
G_{Bj}	the mass of the *Bj* components
$g_j(T_i, M_i)$	the *j*th inequality constraint of performance
G-optimization	the optimization is performed in the global tests
GRA	grey relational analysis
GRA&CV	grey relational analysis and coefficient of variation
GRA&OCV	grey relational analysis and optimized coefficient of variation
GRC	grey relational coefficient
GRG	grey relational grade
HSST	Headrest Static Strength Test
K	the amount of data in a certain sequence
L-optimization	the optimization is performed in the local tests
m_1	the number of simulation results
m_2	the quantity of objective characteristics
M_i	the material type of *i*th component
$Max_t x_i(t)$	the maximum value of the sequence $x_i(t)$
$Min_t x_i(t)$	the minimum value of the sequence of $x_i^*(t)$
MW	an optimization method adopting multi-criterial decision-making methods and weight methods
n	the number of objectives
OCV	optimized coefficient of variation
OLHS	optimal latin hypercube sampling
Optimi-components	components which need to be optimized
P_i	the material price
PFEN	post-fracture elongation
Q	the vector function of performance
r	the number of components
$R_{\partial_i - B_i}$	the ratio of energy absorption to mass of B_i component in ∂_i safety test
S_{Bi}	the plastic strain of *Bi* component
SAT	Seatbelt Anchorage Test
SBST	Seat Back Strength Test
SI_{Bi}	the strain index of *Bi* component
SI_{Bi}^a	the allowable strain index of *Bi* component
SI_{Bi}^l	the strain index of *Bi* component to the limit
$SI_{Bi\cdots Bj}$	the weighted average strain index from *Bi* to *Bj* components
SIGY	yield strength
t	the code of each sequence
T_i	the *i*th component thickness
T_i^D	the lower boundary of component thickness
T_i^U	the upper boundary of component thickness
TOPSIS	technique for order preference by similarity to ideal solution
TOPSIS&CV	technique for order preference by similarity to ideal solution and coefficient of variation
TOPSIS&OCV	technique for order preference by similarity to ideal solution and optimized coefficient of variation
w_t	the *t*th quality characteristic weight
x	the number of material type
$x_i(t)$	the original sequence of simulation results for *i*th element in the *t*th sequence
$x_i^*(t)$	the sequence generated by the grey relation
50 DF/RCPT	50 Dummy Frontal/Rearal Crash Performance Test
50 DFCPT	50 Dummy Frontal Crash Performance Test
50 DRCPT	50 Dummy Rearal Crash Performance Test
∂_i	the codes of safety tests
ρ_i	the density of the material
$\gamma\left(x_r^*(t), x_i^*(t)\right)$	the grey relational coefficient
ω	the difference coefficient
$\overline{a_t}$	the average value of the *t*th sequence
δ_a	the safety factor
δ_t	the coefficient of variation of the *t*th sequence
$\varphi\left(x_r^*, x_i^*\right)$	the value of GRG

1 Introduction

Lightweight optimization of automobile body has been attracted great attention worldwide due to the requirements of energy conservation and automobile safety. However, rare research on the lightweight optimization of the passenger car seat is conducted.

Over the past three decades, fundamental works are conducted on crashworthiness and lightweight optimization for the automobiles. Some researchers devote themselves to the lightweight optimization of vehicle parts, such as Zeng et al. (2016) who improve energy absorption and light the weight of bumper by applying fruit fly optimization algorithm (FOA) in frontal bumper beam. With respect to other parts of a vehicle, readers may refer to Montoya et al. (2015), Wang (2018), Liu et al. (2018), Yin et al. (2018), Zhu et al. (2018), Papaioannou and Koulocheris (2018), Ma et al. (2019), Fossati et al. (2019), Su et al. (2019), etc. Others are conducted on the crashworthiness optimization for cars. Duan et al. (2019) performed multi-objective reliability–based design optimization (RBDO) to the front longitudinal beam and make it more lightweight and crashworthy. With respect to other crashworthiness optimization, readers may refer to Gu et al. (2013), Sun et al. (2017), Lin et al. (2018), Safari et al. (2018), Gao et al. (2019), etc.

However, rare study is carried out for the lightweight optimization of passenger car seat. Kim et al. (2014) studied the fatigue properties of the high-tension steel plate (HTSP) seat frame by experimental validation. Kong et al. (2016) and Zhang et al. (2019) used a topology optimization method to conduct lightweight design for seat frame without reducing the strength and stiffness of the seat. Kong and Cho (2018) designed a sandwich structure as a seat back frame by using composite material. A complete seat design needs to satisfy various safety tests. Currently, most of the studies are focused on the application of either high-strength lightweight materials or the structural optimization with single safety test. Few researchers explicitly proposed detailed methods and design processes for lightweight optimization of passenger car seat for various safety tests. Therefore, in this study, a design process combining the L-optimization (the optimization is performed in the local tests[1]) and G-optimization (the optimization is performed in the global tests[2]) is proposed for the first time, such that the whole safety tests can be satisfied.

Similar to lightweight optimization of automobile body, there are two main evaluation standards during the design of the passenger car seat frame, lightweight and performance, which are mutual exclusive to some extent. Hence, a balance to build between them may be a necessity. The lightweight design of the seat frame should consider the influence of multiple disciplines on its overall aspects (the mass, the vibrational performance, the safety performance, the price, etc.), which is essentially a multi-objective optimization problem (MOOP). In order to solve this problem, scholars had conducted many researches in the past few decades and obtained plenty of effective methods. There are two main optimization methods in multi-objective optimization. One approach is to perform global optimization by using alternative models, optimization algorithms, and weight methods, named as AOW, and the other one is to adopt multi-criterial decision-making methods and weight methods to select the optimal scheme in the sample points, named as MW, as shown in the Fig. 1, where the blocks of the approaches are described below:

- Alternative models: since the number of samples directly affects the efficiency of multi-objective optimization, researchers have widely used alternative models to save computer resources, response surface methodology (RSM) (Fang et al. (2017), Qader et al. (2019), radial basis function (RBF) Wang (2015), Fang et al. (2017), Kriging model (Fang et al. (2017), Choi et al. (2018), etc.
- Optimization algorithms: many optimization algorithms have been developed, such as multi-objective particle swarm optimization algorithm (MOPSO) (Niresh et al. (2019), multi-objective ant colony optimization algorithm (MOACO) (Barán and Laufer (2015), multi-objective genetic algorithm MOGA (Chau et al. (2019), genetic algorithm (GA) (Wang et al. (2018), non-dominated sorting genetic algorithm (NSGA-II) (Han et al. (2019), on-dominated sorting genetic algorithm (NSGA-III) (Yuan et al. (2014) and Qu et al. (2019), etc.
- Multi-criterial decision-making (MCDM): to determine the best compromise for multi-objective optimization, multi-criterial decision-making (MCDM) methods are used: technique for order preference by similarity to ideal solution (TOPSIS) (Xiong et al. (2018a, b), grey relational analysis (GRA) (Fang et al. (2015), Xiong et al. 2018a, b, rank sum ratio (RSR) (Wang et al. (2015), etc.
- Weight methods: in order to determine weights under the multi-objective optimization, the researchers proposed various weight methods: analytic hierarchy process (AHP) (Golbabaie et al. (2019), principal component analysis (PCA) (Pradhan (2013), Zhong et al. (2019), coefficient of variation (CV) (Alharbi et al. (2019), entropy method (EM) (Xiong et al. (2019), etc.

In AOW, most of the available optimization algorithms are only suitable for the situation with small optimization objectives (Xiong et al. (2018a, b) due to the dimensionality and the

[1] Local tests are the tests that focus on the partial components in the passenger car seat frame and include SAT, SBST, HSST, FULT, APT. (These nomenclatures are defined in Section 2.1.)

[2] Global tests are the tests that focus on the all components in the passenger car seat frame and include 50DF/RCPT. (This nomenclature is defined in Section 2.1.)

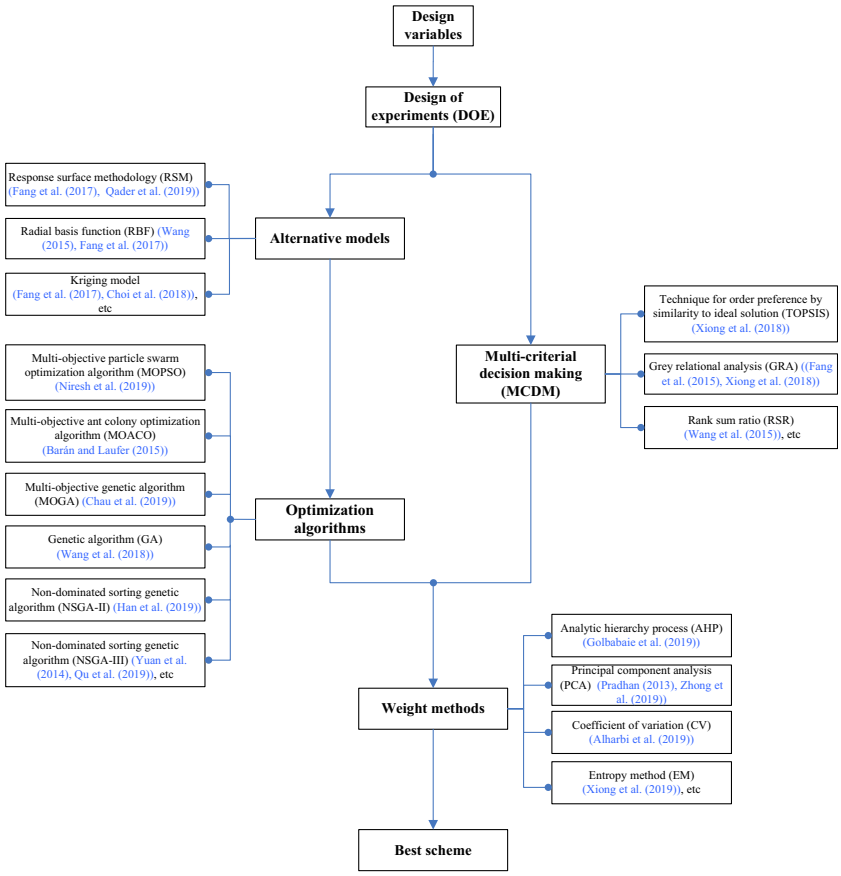

Fig. 1 Two main optimization methods of multi-objective optimization

computation complexity. Meanwhile, in order to maximize the lightweight potential of the seat frame, alternative model is implemented in the multi-objective optimization. To guarantee the high precision of the surrogate model, many experiments need to be conducted, which, however, would be a great challenge due to enormous safety tests. Hence, the optimization methods of AOW are not suitable for the multi-objective optimization of the passenger car seat frame. In MW, the GRA can effectively avoid the above shortcomings and solve the optimization problems with large objectives. The GRA, proposed by Deng, is an algorithm, aiming at solving incomplete, impoverished, and uncertain information problems, and can be applied to handle the relationship among different objectives (Deng 1989). Chen (2019) proposed a new evaluation model through combining grey relational analysis and TOPSIS. Cai and Wang (2017) optimized the automotive S-rail by adopting grey relational analysis and grey entropy measurement to increase performance. Likewise, GRA is also widely applied in vehicles. Baynal et al. (2018) applied the GRA in automotive manufacturing process. Xiong et al. (2018a, b) studied the multi-objective lightweight optimization based on the crashworthiness of side structure of automobile body by using grey relational analysis and principal component analysis. In addition, due to the particularity of the data for optimization objective in seat frame, the traditional weight methods are no longer appropriate to the multi-objective optimization of seat lightweight. The optimized coefficient of variation (OCV) is proposed and can solve this problem, since the optimized range method is utilized which makes the original data dimensionless firstly and then weights the objectives by the coefficient of variation method.

Therefore, in this paper, in order to obtain all aspects of performance simultaneously, L-optimization and G-optimization are adopted in the process of seat frame design. The grey relational analysis and the optimized coefficient of variation (GRA&OCV) are applied in the multi-objective optimization of the passenger car seat frame to provide forward design guidance.

The rest of this study is organized as follows. Section 2 introduces the method, mathematical model, and evaluation criteria for multi-objective lightweight optimization of passenger car seat frame; Section 3 establishes and validates models of the passenger car seat; Section 4 introduces a method to select design variables for lightweight optimization; then Section 5 discusses the design of experiment (DOE) and simulation results of experiments; Section 6 describes the grey relational analysis method, coefficient of variation method, and optimized coefficient of variation method, respectively, and then obtains the best scheme by using the GRA&OCV;

finally, Section 7 compares and verifies the lightweight optimization schemes; Section 8 describes the methods of safety tests; and Section 9 summarizes the study.

2 The method, mathematical model, and evaluation criteria for multi-objective lightweight optimization of passenger car seat frame

2.1 Lightweight optimization method

In this paper, the multi-objective lightweight optimization models, the ratio of energy absorption to mass method, the optimal latin hypercube sampling (OLHS) method, the grey relational analysis and coefficient of variation (GRA&CV), the grey relational analysis and optimized coefficient of variation, TOPSIS and coefficient of variation (TOPSIS&CV), and TOPSIS and optimized coefficient of variation (TOPSIS&OCV) are simultaneously applied into the design of passenger car seat frame for multi-objective lightweight optimization. The passenger car seat safety tests involve Seatbelt Anchorage Test (SAT), Seat Back Strength Test (SBST), Headrest Static Strength Test (HSST), Frame Ultimate Load Test (FULT), Antisubmarine Pan Test (APT), and 50 Dummy Frontal/Rearal Crash Performance Test (50 DF/RCPT). Firstly, the consistency of vibrational and safety performance of the passenger car seat between simulation results and physical experiments results validated the built models. Secondly, different components which need to be optimized (opti-components) are selected by comparing the ratio of energy absorption to mass of seat frame components in different safety tests. SAT, SBST, HSST, FULT, and APT are used to optimize corresponding components for lightweight, and the strain index, the displacement of key points, the material cost, and the total mass of the opti-components are considered four objectives under the L-optimization, while 50 DF/RCPT are used to optimize corresponding components for lightweight, and the strain index, the material cost, and the total mass of the opti-components are considered three objectives under the G-optimization. Thirdly, the design of experiment is performed base on OLHS. Fourthly, the GRA is adopted to optimize the material thickness scheme of the opti-components. The optimized coefficient of variation method is applied to evaluate the corresponding weighting values of the objectives. Finally, the effectiveness of structural and lightweight integrated design is confirmed by the comparison between the original scheme and the optimal scheme. The flowchart of lightweight optimization method is shown in Fig. 2.

There are three parts in the flowchart. The first part is that vibrational and safety performance models are established and validated by comparing simulation results and physical experiments results of passenger seat.

The second part is that the simulation analysis of SAT, SBST, HSST, FULT, and APT is performed in the L-optimization, respectively. The ratio of energy absorption to mass method is used to select lightweight design parts. Next, the OLHS is carried out for DOE. Then, the best thickness-material schemes of lightweight design parts in the passenger seat frame can be obtained through adopting GRA&OCV method. After that, the material thickness schemes are recorded into the 50 DF/RCPT models, and the remaining parts for lightweight design are determined in the global optimization. The same method of optimization is applied in the 50 DF/RCPT.

The third part is that vibrational and safety performance models are updated according to the best schemes. Meanwhile, a comparison is made among the methods of GRA&OCV, GRA&CV TOPSIS&CV, and TOPSIS&OCV. Finally, the effectiveness of lightweight optimized design is verified by GRA&CV, TOPSIS&CV, and TOPSIS&OCV.

2.2 Mathematical model of multi-objective lightweight optimization

Discrete material types and continuous thickness parameters of components are chosen as design variables in the process of multi-objective lightweight optimization of passenger car seat frame. The specified ID numbers are assigned as discrete material types from *1* to *x* and are ordered by yield limit. The material type of *i*th component is defined as a design variable named as M_i, and its mathematical model is expressed as follows (Xiong et al. (2018a, b):

$$\begin{pmatrix} \rho_i \\ E_i \\ P_i \\ \vdots \end{pmatrix} = \begin{pmatrix} f_\rho(M_i) \\ f_E(M_i) \\ f_P(M_i) \\ \vdots \end{pmatrix} \tag{1}$$

where x is the number of material type, ρ_i is the density of the material which is expressed by $f_\rho(M_i)$, E_i is the material elastic modulus expressed by $f_E(M_i)$, and P_i is the material price demonstrated by $f_P(M_i)$.

The multi-objective optimization mathematical model of passenger car seat material thickness is:

$$\begin{aligned} &Minimize\ G = G(T_i, \rho_i) = \textstyle\sum_{i=1}^{z} A_i T_i \rho_i \\ &= G\Big(T_i, f_\rho(M_i)\Big) = G(T_i, M_i), i = 1, 2, 3, \cdots, r \end{aligned} \tag{2}$$

$$\begin{aligned} &Minimize\ Q \\ &= (\min Q_1(T_i, M_i), \min Q_2(T_i, M_i), \cdots, \min Q_n(T_i, M_i)), i \\ &= 1, 2, 3, \cdots, r \end{aligned} \tag{3}$$

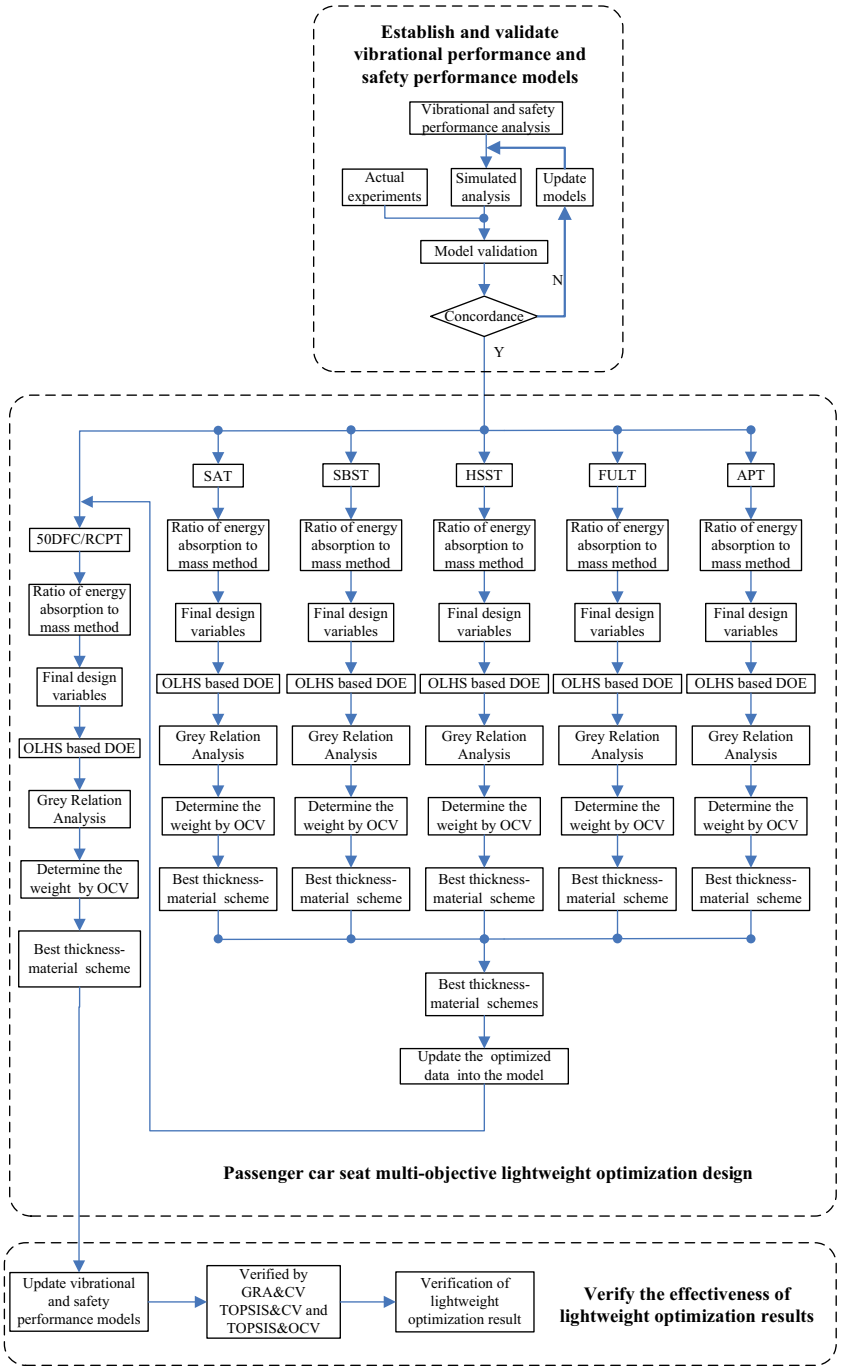

Fig. 2 Flowchart of lightweight optimization method

$$\begin{aligned} &Minimize\ C = C(T_i, \rho_i, P_i) = \sum_{i=1}^{z} A_i T_i \rho_i P_i \\ &= C\left(T_i, f_\rho(M_i)\right) = C(T_i, M_i), i = 1, 2, 3, \cdots, r \end{aligned} \tag{4}$$

$$\text{s.t.} \begin{cases} g_j(T_i, M_i) \le 0, i = 1, 2, 3, \cdots z, j = 1, 2, 3, \cdots, e \\ T_i^D \le T_i \le T_i^U, i = 1, 2, 3, \cdots r \\ M_i \in \{1, 2, 3, \cdots n\}, i = 1, 2, 3, \cdots r \end{cases} \tag{5}$$

where A_i represents the ith component area, T_i is the ith component thickness, r is the number of components, e is the number of inequality constraints, T_i^D and T_i^U are the lower and upper boundary of component thickness, G is the total mass of passenger car seat frame, Q is the vector function of performance, C is the cost of material, and $g_j(T_i, M_i)$ is the jth inequality constraint of performance.

Because the above mathematical model is a multi-objective nonlinear problem with discrete and continuous variables, the grey relational analysis method and the optimized coefficient

of variation method are applied to get the material and thickness optimal matching scheme of the opti-components in this paper.

2.3 Evaluation criteria

Similar to the automobile body lightweight optimization, the seat lightweight optimization has three criteria: performance, weight, and cost. According to the seat industry standards, the first-order vibrational frequency must be greater than 18 Hz. Hence, the first-order vibrational frequency is one of the performance criteria. Based on international seat safety standards, the displacement of a certain part should be less than a certain threshold in some safety test and can be replaced by the displacement of key points on the parts. So, the displacement of key measurement points is also one of the performance criteria. Meanwhile, all parts of the seat frame should not fail except APT. Therefore, the strain index is proposed to determine whether a part has failed. As a result, the strain index of components is one of the performance criteria, while the lightweight criterion is the total weight of seat frame, and the economic criterion is the cost of the total cost of the opti-components.

The strain index of components can be calculated as follows:

$$S_{Bi} = \frac{SI_{Bi}}{E_{Bi}} \tag{6}$$

where *Bi* represents the codes of components, SI_{Bi} is the strain index of *Bi* component, S_{Bi} is the plastic strain of *Bi* component, and E_{Bi} is the post-fracture elongation of material of *Bi* component. In general, a strain index of 1 to the limit is the critical value to judge whether a component is failed. An allowable strain index is used instead of the original one by introducing a safety factor with $SI^a_{Bi} = \frac{SI^l_{Bi}}{\delta_a}$, where SI^l_{Bi} is a strain index of *Bi* component to the limit (in this paper, the strain index to the limit is 1), SI^a_{Bi} is the allowable strain index of *Bi* component, and δ_a is the safety factor. To leave a reasonable design margin, we set the safety factor at 1.053 (1/0.95). When the strain index is greater than 0.95, the component is considered disabled, otherwise, normal. If two or more opti-components appear in a safety test, the strain index is decided by the average weighting method as follows:

$$SI_{Bi\cdots Bj} = \frac{SI_{Bi}G_{Bi} + \cdots + SI_{Bj}G_{Bj}}{G_{Bi} + \cdots + G_{Bj}} \tag{7}$$

where $SI_{Bi\cdots Bj}$ denotes the weighted average strain index from *Bi* to *Bj* components and G_{Bi} and G_{Bj} represent the mass of the *Bi* and *Bj* components, $i = 1, 2, 3, \cdots 11$, $j = 1, 2, 3, \cdots, 11$.

The evaluation criteria of passenger car seat include (1) the first-order vibrational frequency; (2) the displacement of key measurement points and the strain index of opti-components; (3) the total mass of the seat frame; and (4) the total cost of the opti-components. In this study, the key measurement points are selected under the safety tests. As shown in Fig. 3, the A_1, D_1, L_1, O_1, and R_1 are selected in the SAT, SBST, HSST, FULT, and APT, while the A_1 represents the midpoint of rail buckle, the D_1 represents the fixed point of backrest side member, L_1 represents the midpoint of headrest tube, O_1 represents the midpoint of

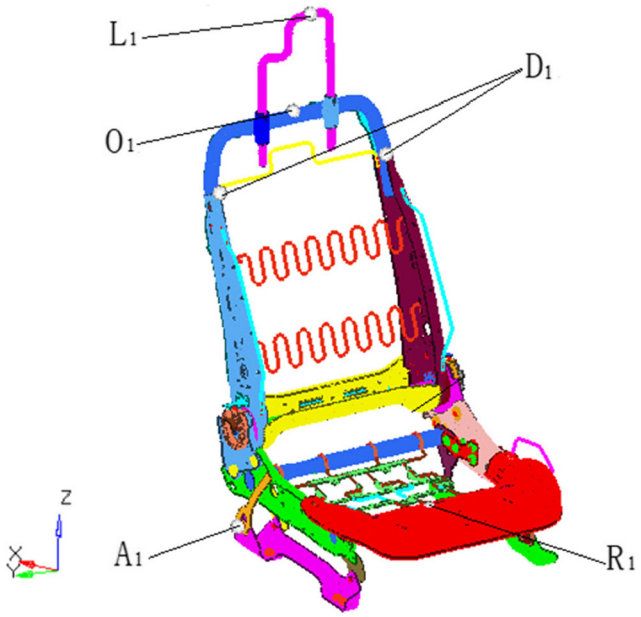

Fig. 3 Performance measurement points of passenger car seat frame

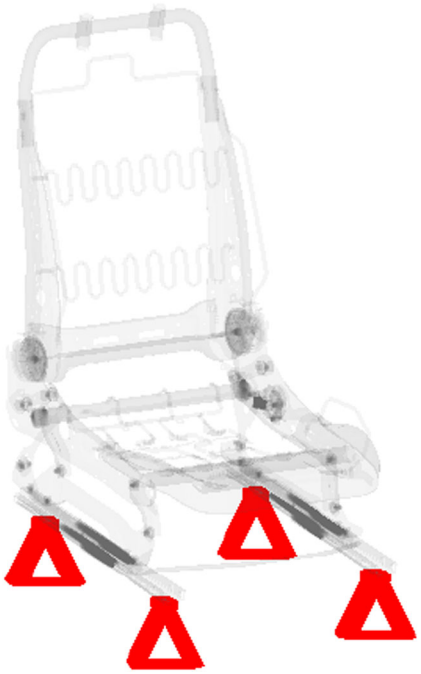

Fig. 4 Vibrational model

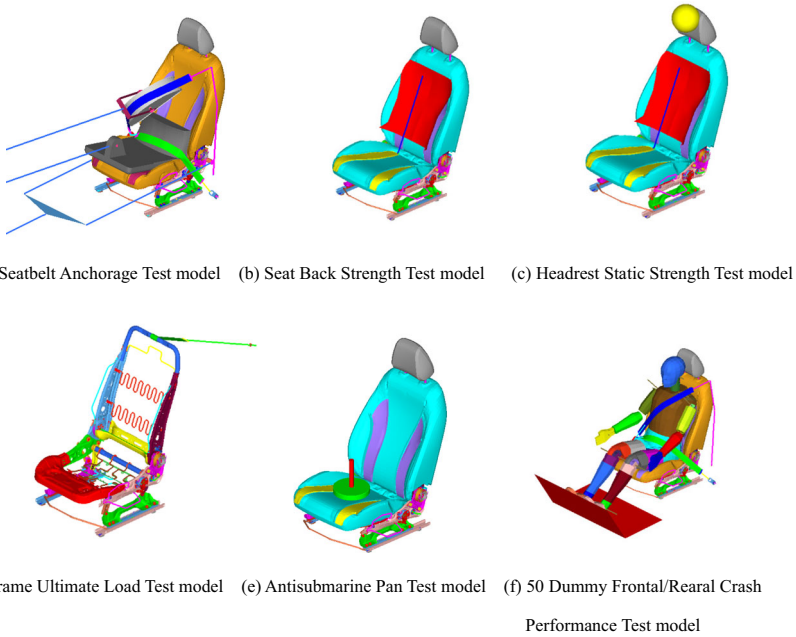

(a) Seatbelt Anchorage Test model (b) Seat Back Strength Test model (c) Headrest Static Strength Test model

(d) Frame Ultimate Load Test model (e) Antisubmarine Pan Test model (f) 50 Dummy Frontal/Rearal Crash Performance Test model

Fig. 5 Safety performance models of passenger car seat

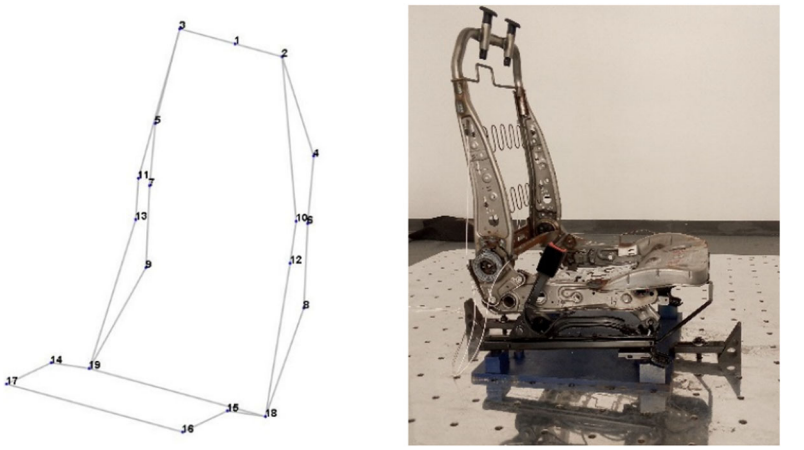

(a) Sensor arrangement point (b) State diagram of passenger car seat

Fig. 6 Physical vibrational experiment

backrest upper square tube, and R_1 represents the midpoint of seatframe front tube. Meanwhile, the SA_1 is the XZ-direction displacement of measurement points A_1 when the load reaches 13,500 N ± 200 N in SAT; the SD_1 is the XZ-direction displacement of measurement points D_1 when the torque reaches 1500 Nm in SBST; the SL_1 is the XZ-direction displacement of measurement points L_1 when the torque reaches 373 Nm in HSST; the SO_1 is the XZ-direction displacement of measurement points O_1 when the torque reaches 1500 Nm in FULT; and the SR_1 is the XZ-direction displacement of measurement points R_1 when the static force reaches 15,000 N in APT. All passenger car seat evaluation criteria are calculated and recorded as shown in Tables 35 and 36 at the end of this paper.

3 Establishment and validation

3.1 Vibrational and safety performance models

According to international safety standards,[3] all relevant performance of the passenger car seat frame should be considered during lightweight design. Therefore, the

[3] The international safety standards are described specifically in Section 8.

(a) Seatbelt Anchorage Test (b) Seat Back Strength Test (c) Headrest Static Strength Test

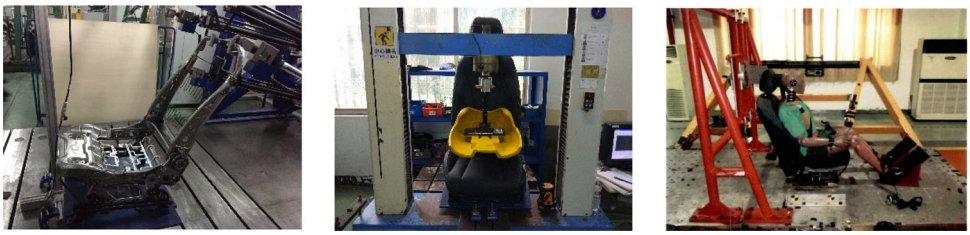

(d) Frame Ultimate Load Test (e) Antisubmarine Pan Test (f) 50 Dummy Frontal/Rearal Crash Performance Test

Fig. 7 All safety performance actual experiments of passenger car seat

Table 1 Vibrational analysis (unit: Hz)

Vibrational hierarchy	Vibrational shape	Simulation	Experiment	Error (%)
1	First-order transverse vibration of backrest	27.75	28.89	3.95
2	First-order longitudinal vibration of backrest	35.67	33.77	−5.63
3	Global torsion of seat	42.35	44.66	5.17

accurate FEA (Finite Element Analysis) models of the vibrational and safety performance for passenger car seat are indispensable. The vibrational performance of passenger car seat frame is mainly shown through the low-order vibrational frequencies below 50 Hz; the vibrational simulation model is shown in Fig. 4. Figure 5 presents the FEA models of all safety tests including the Seatbelt Anchorage Test model (Fig. 5a), the Seat Back Strength Test model (Fig. 5b), the Headrest Static Strength Test model (Fig. 5c), the Frame Ultimate Load Test model (Fig. 5d), the Antisubmarine Pan Test model (Fig. 5e), and the 50 Dummy Frontal/Rearal Crash Performance Test model (Fig. 5f).

3.2 Simulation and physical experiment of models

The corresponding physical experiments are carried out to validate the accuracy and effectiveness of the abovementioned FEA models. Figure 6a denotes the sensor arrangement point in the physical vibrational experiment, Fig. 6b denotes the passenger car seat state diagram in the physical vibrational experiment, and Fig. 7 shows the physical safety performance experiments of the passenger car seat. Table 1 shows both the vibrational results of simulation and experiment. It can be seen that the results of simulation and experiment are approximately the same. The errors of the low-order vibrational frequencies are respectively 3.95%, −5.63%, and 5.17%. The results indicate that the model can really reflect the vibration characteristics of the seat frame.

Meanwhile, in order to compare the simulation with the physical experiment results of all safety tests in detail, X-direction, Z-direction, or XZ-direction[4] displacement characteristics w.r.t. time of key measurement point of every safety test is selected for comparison (Fig. 8). As shown in Fig. 8, it can be seen from the displacement curve that the results of experiment are approximately consistent with the simulation, except for some small errors in time and phase. In addition, the results from the simulation in the trend, the peak values, and

[4] [2]The XZ-direction displacement of one point represents its displacement on the XZ-plane, in more detail, $\sqrt{X^2 + Z^2}$.

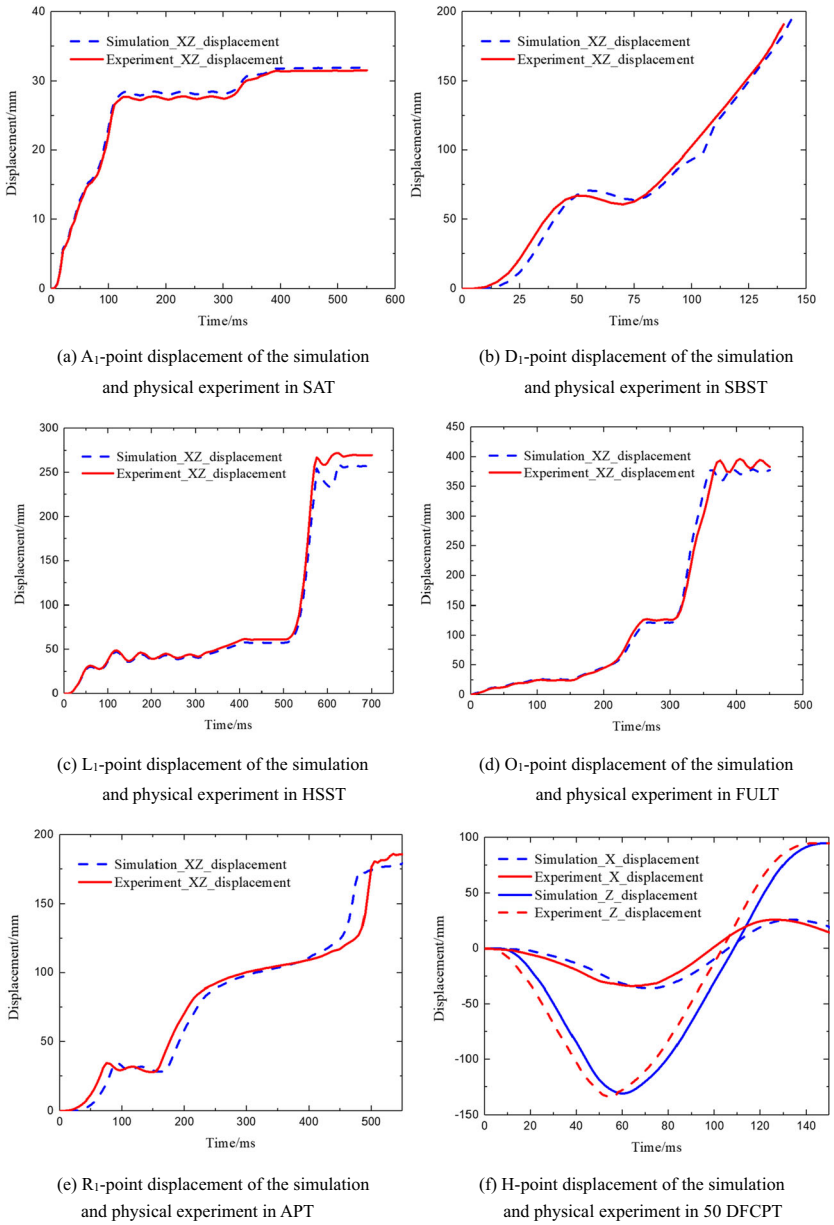

(a) A_1-point displacement of the simulation and physical experiment in SAT

(b) D_1-point displacement of the simulation and physical experiment in SBST

(c) L_1-point displacement of the simulation and physical experiment in HSST

(d) O_1-point displacement of the simulation and physical experiment in FULT

(e) R_1-point displacement of the simulation and physical experiment in APT

(f) H-point displacement of the simulation and physical experiment in 50 DFCPT

Fig. 8 All key measurement points displacement of the simulation and physical experiment in safety tests

the amplitude of curve are similar to those form the experiments. Therefore, the vibrational and safety performance models built in this paper can be applied for the following optimization.

4 Design variables of lightweight optimization

4.1 Ratio of energy absorption to mass method

There are a number of dynamic safety tests need to be conducted at the same time in the process of designing passenger car seats. Since several decades, it is of difficulty for seat frame to perform lightweight optimization simultaneously under all safety tests. How to balance the performances of all safety tests is of great significance. Hence, this paper adopts L-optimization and G-optimization to carry out the multi-objective lightweight optimization of seat frame. The SAT, SBST, HSST, FULT, and APT are consisted in L-optimization, while the 50 DF/RCPT is consisted in G-optimization. The traditional sensitivity analysis method (Chen and Zuo (2014), Zuo et al. (2016) is limited to linear analysis, and the method of contribution analysis based on collision is too complicated (Xiong et al. 2018a, b). Meanwhile, the

components of seat frame are few and symmetrically distributed. Therefore, in order to solve this challenge, the ratio of energy absorption to mass method is proposed as a direction method to determine finial lightweight design components of the seat frame. The specific method is as follows:

Step 1. Simulation analysis is carried out for all safety tests.
Step 2. Energy absorption and mass of components are derived on every safety test.

$$R_{\partial_i - B_i} = \frac{E_{\partial_i - B_i}}{G_{B_i}} \tag{8}$$

where ∂_irepresents the codes of safety tests, $R_{\partial_i - B_i}$ is the ratio of energy absorption to mass of B_i component in ∂_i safety test, $E_{\partial_i - B_i}$ is the energy absorption value of B_i component in ∂_i safety test, and G_{B_i} is the mass of B_i component.

Step 3. Through comparing the values of ratio of energy absorption to mass for different parts, the components which have bigger value of ratio are selected as lightweight design components to optimize in the same safety test.

4.2 Design variables

For simplicity, 15 parts are originally selected and marked from B1 to B15 (Fig. 9). Such as headrest tube, backrest upper square tube, backrest side member, backrest recliner lower bracket, inner and outer rails, etc.

In this paper, it is found that the values of ratio for some components are much larger than the other components through comparing the values of ratio of energy absorption to mass under all safety tests (Fig. 10). To be more specific, the part B1 with the largest ratio value in the SAT (Fig. 10a) is selected as optimization component. Similarly, the ratio values of the parts B2, B3, and B4 are determined as optimization component, respectively, in the SBST (Fig. 10b), the HSST (Fig. 10c), and the FULT (Fig. 10d); the ratio values of the parts B5 and B6 are much larger than other parts, and thus the parts B5 and B6 are selected as optimization component in the APT (Fig. 10e). Likewise, the 50 DF/RCPT (Fig. 10f), in which the ratio values of parts are arranged from large to small, has more optimizable parts which have top five ratio values leading to the parts B7, B8, B9, B10, and B11which are selected as opti-components. Finally, 11 components are selected from seat frame, whose thicknesses are defined as design variables marked from T1 to T11 and corresponding material types are defined as design variables marked from M1 to M11 (Fig. 11).

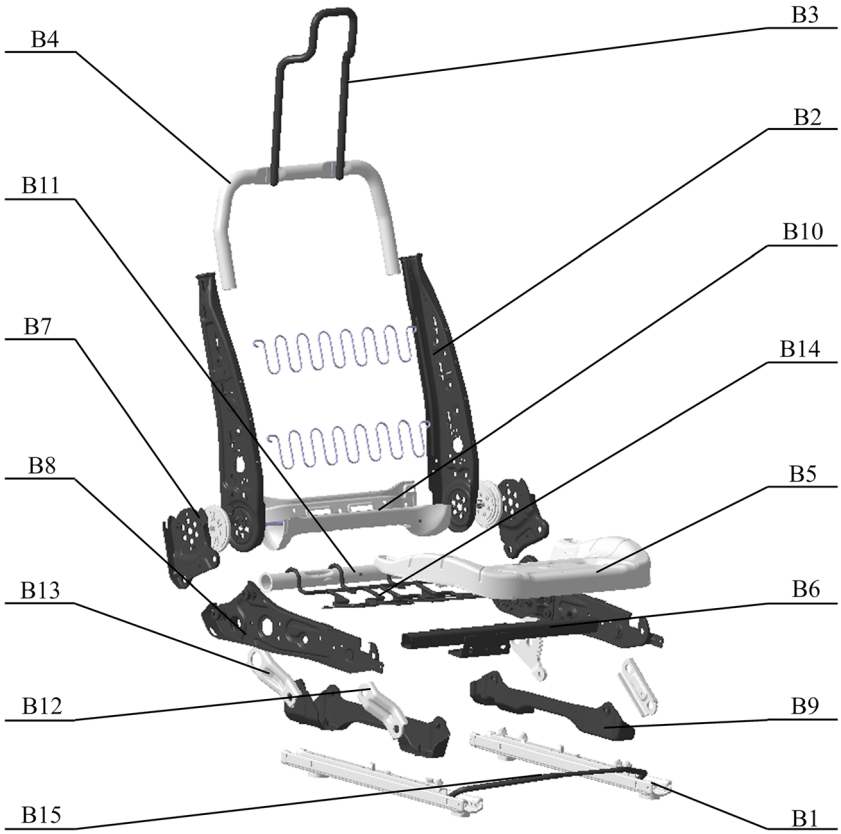

Fig. 9 Main stressed components of passenger car seat

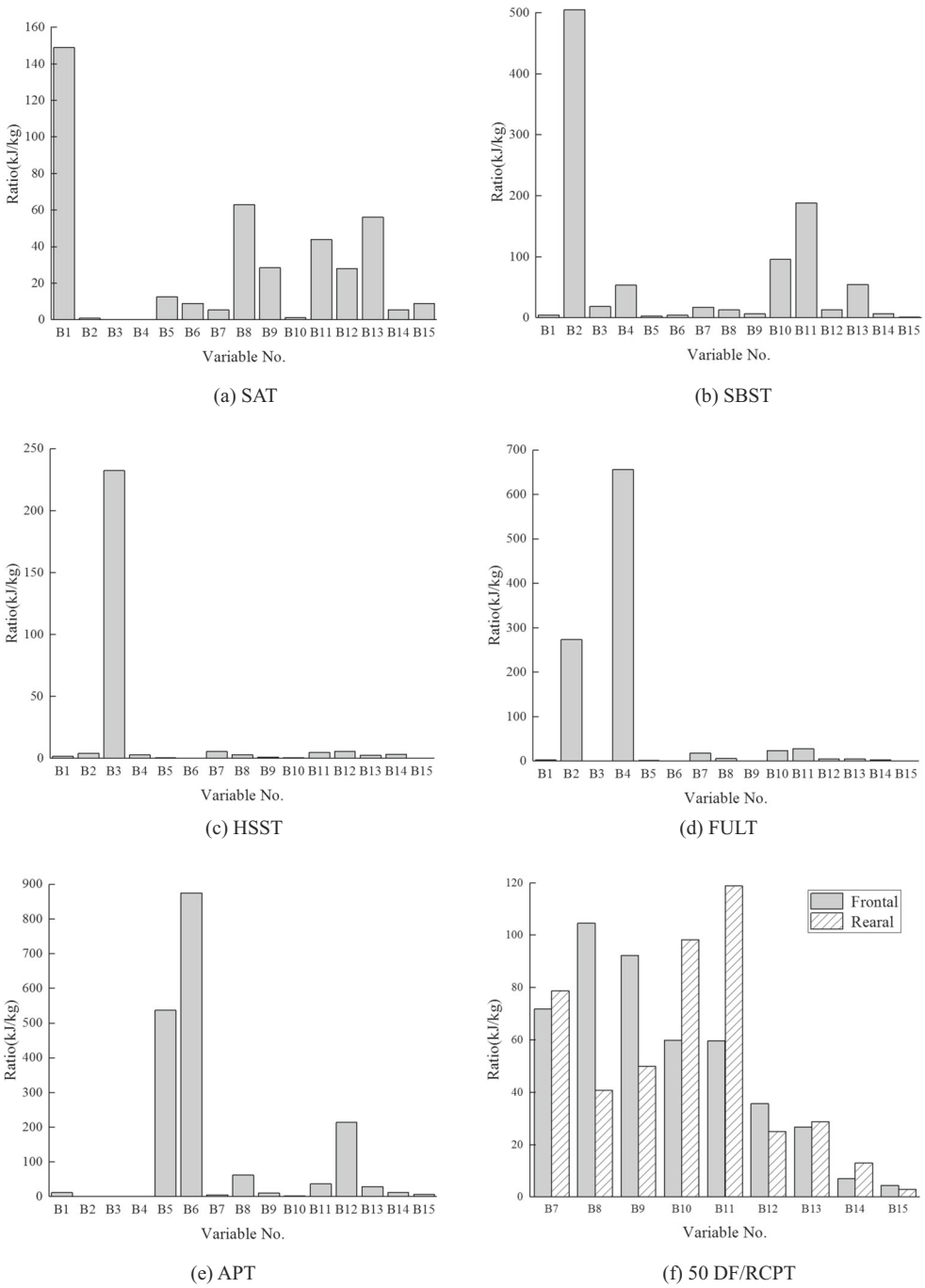

Fig. 10 Ratio of energy absorption to mass of design variables

5 DOE for lightweight optimization

5.1 Experimental parameters

Fourteen material variables and 11 thickness variables are selected as the final design variables, namely, the experiment parameters. Specifically, the "Original value" column and the "Original level" column represent the thickness and material type of the opti-components in original design; the "Experimental range" column and the "Experimental level" denote the range of thickness and material type of the opti-components. The thickness variables of opti-components except the part B1 are 60–140% of the original components, and the material variables of opti-components except the part B1 are range of 9 experimental levels in Table 2; the optimization thickness of part B1 is 60%–120% of the original thicknesses, and its material variable is 5 experimental levels. In this paper, 14 candidate material types are defined as 101 to 114 in turn according to the increased values of yield strength

Fig. 11 Final design variables of lightweight optimization

and are correspondingly given the Poisson ratio, elastic modulus, density, yield strength (SIGY), post-fracture elongation (PFEN), and material costs of candidate materials as shown in Table 3. In this paper, the true stress-strain curves are matched according to the physical tests of materials.

5.2 Experimental design and simulation results of experiment

According to different seat safety tests, different thicknesses and material types of components are selected. The optimal combination scheme of thickness and material parameter is obtained by repeating the seat safety tests using the OLHS. According to the OLHS standard, the minimum sample size is $\frac{(a+1)(a+2)}{2}$ (Fang et al. 2017), where a is the number of design variables. In the SAT, SBST, HSST, and FULT, the number of design variables is 2 and the minimum sample size is 6, while in the APT and 50 DF/RCPT, the numbers of design are 4 and 10 and the minimum sample sizes are 15 and 66. In order to acquire experimental results with more details and fully consider the material types and the thickness ranges, 25 experimental samples are designed for the SBST, HSST, and FULT, and 15 experimental samples are designed for the SAT which has less level of design variable than the SBST, HSST, and FULT, while 40 and 100 experimental samples listed in Table 4 are designed for the APT and 50 DF/RCPT, respectively.

According to the standard, failure of every component is not allowed under any safety tests expect APT, namely, the strain index must be less than 1. So, in this paper, the simulation results of the component with the strain index greater than 0.95 (safety factor is 1/0.95) are eliminated when analyzing the results. If the amount of optimization component is greater than one, the strain index can be calculated by formula (7). The simulation results of the SAT, SBST, HSST, FULT, APT, 50 DFCPT, and 50 DRCPT are shown in Tables 5, 6, 7, 8, 9, 10, and 11. 12 shows the weights of components from B7 to B11; then the weighted average strain index of 50 DFCPT and 50 RFCPT can be obtained by using the formula (7) shown in Table 13.

5.3 Optimization objectives

Various performance criteria should be considered in the process of the lightweight optimization of the seat. Usually, the strain index of components and the displacement of key measurement points are applied to assess the safety level. In

Table 2 Experimental parameter ranges

Thickness variable	Original value (mm)	Experimental range (%)	Material variable	Original level	Experimental level
T1	1.8	60–120	M1	110	110–114
T2	1.2	60–140	M2	109	105–113
T3	1.5	60–140	M3	103	101–109
T4	1.2	60–140	M4	107	103–110
T5	0.8	60–140	M5	101	101–109
T6	1.2	60–140	M6	109	105–113
T7	3	60–140	M7	110	106–114
T8	1.8	60–140	M8	110	106–114
T9	3	60–140	M9	108	104–112
T10	0.8	60–140	M10	109	105–113
T11	1.6	60–140	M11	106	102–110

Table 3 Candidate materials

Material no.	Material name	Poisson ratio	Elastic modulus (MPa)	Density (kg/m^{-3})	SIGY (MPa)	PFEN (%)	Material cost (¥/kg)
101	DC01	0.3	2.1E + 05	7.85E + 03	195	0.270	3.90
102	Q195	0.3	2.1E + 05	7.85E + 03	195	0.278	4.06
103	Q235	0.3	2.1E + 05	7.85E + 03	235	0.223	4.25
104	SAPH400	0.3	2.1E + 05	7.85E + 03	255	0.278	4.11
105	SAPH440	0.3	2.1E + 05	7.85E + 03	305	0.262	4.31
106	QSTE340TM	0.3	2.1E + 05	7.85E + 03	340	0.191	4.48
107	Q345	0.3	2.1E + 05	7.85E + 03	345	0.199	4.56
108	QSTE420TM	0.3	2.1E + 05	7.85E + 03	420	0.191	4.72
109	B410LA	0.3	2.1E + 05	7.85E + 03	485	0.157	4.84
110	S500MC	0.3	2.1E + 05	7.85E + 03	500	0.113	4.79
111	HC500	0.3	2.1E + 05	7.85E + 03	500	0.095	5.01
112	S550MC	0.3	2.1E + 05	7.85E + 03	550	0.113	4.95
113	H800LA	0.3	2.1E + 05	7.85E + 03	780	0.086	5.20
114	D1000DPX	0.3	2.1E + 05	7.85E + 03	850	0.060	5.45

Table 4 The number of samples and selection of opti-components

Safety tests	Optimization parts	Optimization of types	Key measurement points	Number of samples
SAT	B1	L-optimization	A_1	15
SBST	B2	L-optimization	D_1	25
HSST	B3	L-optimization	L_1	25
FULT	B4	L-optimization	O_1	25
APT	B5/B6	L-optimization	R_1	40
50 DFCPT	B7/B8/B9/B10/B11	G-optimization	●	100
50 DRCPT	B7/B8/B9/B10/B11	G-optimization	●	100

addition, the total mass of the seat frame is used to evaluate the lightweight level, and the total material cost of the opti-components is adopted to evaluate the economic criteria. Therefore, in this paper, four objectives are selected in the L-optimization, including the strain index of components, the displacement of key measurement points, the total mass of the opti-components, and the total material cost of the opti-components. Three objectives are applied in the G-optimization, including the strain index of components, the total mass of the components, and the total material cost of the opti-components. The specific objectives are as follows: (1) the strain index, the total mass, and the material cost of the part B1 and the XZ-direction displacement of the buckle mid-point A_1 are taken as the optimization objectives in the SAT. (2) The strain index, the total mass, and the material cost of the part B2 and XZ-direction displacement of fixed point D_1 are

Table 5 SAT simulation layout and results

No.	Simulation layout		Simulation results			
	M1	T1/mm	SI_{B1}	SA_1/mm	G/kg	Cost/¥
1	113	2.160	0.341	25.075	3.134	16.297
2	110	1.929	0.702	31.588	2.798	13.402
3	113	1.851	0.462	27.607	2.687	13.972
4	111	1.697	0.649	37.570	2.463	12.340
…	…	…	…	…	…	…
15	114	1.620	0.635	30.223	2.351	12.813

Table 6 SBST simulation layout and results

No.	Simulation layout		Simulation results			
	M2	T2/mm	SI_{B2}	SD_1/mm	G/kg	Cost/¥
1	113	1.239	0.012	166.324	1.320	5.886
2	108	1.160	0.437	170.255	1.059	4.998
3	111	1.119	0.211	168.000	1.022	5.120
4	109	1.479	0.022	166.262	1.351	6.539
…	…	…	…	…	…	…
25	112	0.999	0.842	172.733	0.913	4.519

Table 7 HSST simulation layout and results

No.	Simulation layout		Simulation results			
	M3	T3/mm	SI_{B3}	SL_1/mm	G/kg	Cost/¥
1	104	1.249	0.715	80.273	0.269	1.105
2	105	1.699	0.530	38.648	0.366	1.576
3	102	1.900	0.544	38.387	0.409	1.659
4	107	1.600	0.454	39.941	0.344	1.569
25	106	0.949	0.946	61.344	0.204	0.915

taken as the optimization objectives in the SBST. (3) The strain index, the total mass, and the material cost of the part B3 and the XZ-direction of the midpoint L_1 are taken as the optimization objectives in the HSST. (4) The strain index, the total mass, and the material cost of the part B4 and the XZ-direction of the midpoint O_1 are taken as the optimization objectives in the FULT. (5) The strain index, the total mass, and the material cost of the parts B5, B6, and the XZ-direction of the midpoint R_1 are taken as the optimization objectives in the APT. (6) The weighted average strain index of 50 DFCT, the weighted average strain index of 50 DRCT, the material cost, and the total mass of the opti-components are applied as the optimization objectives in the 50 DF/RCPT. The key measurement points under each safety test are shown in Table 4. The total cost of the above materials only represents the prices of raw and semifinished materials and is only judged by the thickness and material type of the components.

6 Data analysis

The purpose of this study is to minimize the strain index of components, the displacement of key measurement points under each safety test, the total mass of passenger car seat frame, and the total material cost of opti-components. However, those four objectives of seat design are difficult to be met at the same time. Therefore, grey relational analysis is applied to solve this problem; the GRA can solve the complex and uncertain multi-objective optimization problems effectively.

Table 8 FULT simulation layout and results

No.	Simulation layout		Simulation results			
	M4	T4/mm	SI_{B4}	SO_1/mm	G/kg	Cost/¥
1	108	1.280	0.104	69.652	0.507	2.394
2	103	1.520	0.903	125.131	0.602	2.560
3	111	0.999	0.551	79.347	0.396	1.985
4	106	1.599	0.029	64.843	0.634	2.840
25	109	1.080	0.684	86.357	0.428	2.071

Table 9 APT simulation layout and results

No.	Simulation layout				Simulation results		
	M5	T5/mm	M6	T6/mm	SR_1/mm	G/kg	Cost/¥
1	107	1.103	106	1.409	111.264	1.687	7.658
2	106	0.775	112	0.991	117.116	1.185	5.442
3	109	0.972	111	1.089	111.982	1.442	7.033
4	103	1.123	107	1.335	114.658	1.684	7.277
40	102	0.923	106	1.630	114.382	1.540	6.447

6.1 Grey relational analysis method

GRA is a multifactor statistical analysis method proposed by Deng in 1982 (Deng (1982). Different formulas are selected according to the actual objective and direction in this method. During the data pretreatment process, the original sequences are converted into comparable sequences and the simulation results can be normalized within the range from 0 to 1. According to the objective characteristics of the original sequence, several different formulas can be used in GRA. Specifically, if the optimal value of original sequence is the minimum, the characteristic of the original sequence is "the smaller, the better," and the original sequence may be normalized as below (Pradhan (2013):

$$x_i^*(t) = \frac{Max_t x_i(t) - x_i(t)}{Max_t x_i(t) - Min_t x_i(t)} \tag{9}$$

Table 10 50 DFCPT simulation layout and results

No.	Simulation layout				Simulation results				
	M7	T7/mm	M11	T11/mm	SI_{B7}	SI_{B8}	SI_{B9}	SI_{B10}	SI_{B11}
1	109	3.497	106	2.227	0.008	0.086	0.381	0.226	0.047
2	106	3.085	107	1.749	0.066	0.191	0.812	0.273	0.000
3	110	2.115	106	2.149	0.028	0.195	0.295	0.241	0.069
4	108	2.575	110	1.826	0.062	0.421	0.563	0.309	0.144
5	110	2.333	102	0.972	0.037	0.232	0.558	0.232	0.045
6	108	1.872	103	2.214	0.045	0.164	0.195	0.236	0.090
7	111	3.957	106	2.240	0.005	0.134	0.140	0.179	0.053
8	107	2.866	105	1.270	0.066	0.403	0.298	0.229	0.117
9	111	2.939	108	1.037	0.039	0.269	0.809	0.305	0.106
10	112	2.187	106	1.115	0.085	0.048	0.163	0.202	0.217
100	114	4.151	107	1.774	0.000	0.070	0.163	0.169	0.055

Table 11 50 DRCPT simulation layout and results

No.	Simulation layout				Simulation results				
	M7	T7/mm	M11	T11/mm	SI_{B7}	SI_{B8}	SI_{B9}	SI_{B10}	SI_{B11}
1	109	3.497	106	2.227	0.056	0.045	0.325	0.133	0.217
2	106	3.085	107	1.749	0.180	0.142	0.466	0.117	0.156
3	110	2.115	106	2.149	0.856	0.225	0.337	0.167	0.115
4	108	2.575	110	1.826	0.290	0.330	0.232	0.116	0.485
5	110	2.333	102	0.972	0.063	0.155	0.278	0.112	0.154
6	108	1.872	103	2.214	0.822	0.116	0.163	0.115	0.179
7	111	3.957	106	2.240	0.055	0.195	0.203	0.153	0.072
8	107	2.866	105	1.270	0.186	0.279	0.151	0.117	0.224
9	111	2.939	108	1.037	0.087	0.335	0.477	0.125	0.178
10	112	2.187	106	1.115	0.298	0.100	0.224	0.170	0.253
100	114	4.151	107	1.774	0.000	0.044	0.244	0.132	0.121

where $x_i^*(t)$ represents the sequence generated by the grey relation, $x_i(t)$ is the original sequence of simulation results for ith element in the tth sequence, $Max_t x_i(t)$ is the maximum value of the sequence $x_i(t)$, $Min_t x_i(t)$ is the minimum value of the sequence of $x_i^*(t)$, $i = 1, 2, 3...m_1$ and $t = 1, 2, 3,...m_2$, m_1 are the numbers of simulation results, and m_2 is the quantity of objective characteristics.

If the optimal value of original sequence is the maximum, the characteristic of the original sequence is "the larger, the better", and the original sequence can be normalized as below:

$$x_i^*(t) = \frac{x_i(t) - Min_t x_i(t)}{Max_t x_i(t) - Min_t x_i(t)} \tag{10}$$

Table 12 50 DF/RCPT weight results

No.	Thickness and material				Weight (kg)				
	M7	T7/mm	M11	T11/mm	G_{B7}	G_{B8}	G_{B9}	G_{B10}	G_{B11}
1	109	3.497	106	2.227	0.766	1.555	1.352	0.376	0.633
2	106	3.085	107	1.749	0.675	1.167	0.899	0.381	0.497
3	110	2.115	106	2.149	0.463	0.905	1.329	0.454	0.611
4	108	2.575	110	1.826	0.564	0.761	1.307	0.246	0.298
5	110	2.333	102	0.972	0.888	1.104	0.887	1.249	0.625
6	108	1.872	103	2.214	0.410	1.058	1.443	0.367	0.629
7	111	3.957	106	2.240	0.867	0.977	1.624	0.373	0.636
8	107	2.866	105	1.270	0.628	0.770	1.692	0.357	0.361
9	111	2.939	108	1.037	0.644	0.860	0.944	0.400	0.295
10	112	2.187	106	1.115	0.479	1.329	1.567	0.446	0.317
100	114	4.151	107	1.774	0.909	1.564	1.499	0.324	0.504

If the optimal value of original sequence is the target value, the original sequence can be normalized as below:

$$x_i^*(t) = 1 - \frac{|x_i(t) - A|}{MAX\{Max_t x_i(t) - A,\quad A - Min_t x_i(t)\}} \tag{11}$$

where A is the target value.

In this research, the displacements of key measurement points in each safety test, the strain index of components, and the total mass and material cost of opti-components should be minimized. Therefore, formula (9) is adopted to normalize the original sequence and the simulation results are normalized to [0,1] (Tables 14, 15, 16, 17, 18, and 19). The reference sequence, to which the normalized results should be as close as possible, normally defined as 1, means the best performances. Accordingly, in this study, the closer the comparable sequence is to the reference sequence, the better the performance will be.

The relationship between comparable sequence and reference sequence can be determined by grey relational coefficient (GRC). The GRC can be deduced as below:

$$\gamma\left(x_r^*(t), x_i^*(t)\right) = \frac{\Delta_{min} + \omega\Delta_{max}}{\Delta_{ri}(t) + \omega\Delta_{max}} \tag{12}$$

where $\gamma\left(x_r^*(t), x_i^*(t)\right)$ represents the grey relational coefficient, ω is the difference coefficient, $\omega \in [0,1]$, and usually takes the value of 0.5; $\Delta_{ri}(t)$, Δ_{min}, and Δ_{max} can be given by:

$$\Delta_{ri}(t) = \left|x_r^*(t) - x_i^*(t)\right| \tag{13}$$

$$\Delta_{min} = \underbrace{\min}_{\forall i}\ \underbrace{\min}_{\forall t}\ \Delta_{ri}(t) \tag{14}$$

$$\Delta_{max} = \underbrace{\max}_{\forall i}\ \underbrace{\max}_{\forall t}\ \Delta_{ri}(t) \tag{15}$$

Formula (12) is used to convert the normalized results into GRC (Tables 22, 23, 24, 25, 26, and 27). The grey relational grade (GRG) can be calculated by using the GRC. In general, the GRG is the average of GRC, and it can be expressed as follows:

$$\varphi\left(x_r^*, x_i^*\right) = \frac{1}{n}\sum_{t=1}^{n}\gamma\left(x_r^*(t), x_i^*(t)\right) \tag{16}$$

If the importance of objective characteristics is different, the following formula can be used to calculate the GRG:

$$\varphi\left(x_r^*, x_i^*\right) = \sum_{t=1}^{n} w_t\gamma\left(x_r^*(t), x_i^*(t)\right) \tag{17}$$

Table 13 50 DF/RCPT simulation layout and results

No.	Simulation layout				Simulation results			
	M7	T7/mm	M11	T11/mm	FC-$SI_{B7...B11}$	RC-$SI_{B7...B11}$	G/kg	Cost/¥
1	109	3.497	106	2.227	0.165	0.158	4.681	21.440
2	106	3.085	107	1.749	0.305	0.229	3.619	16.560
3	110	2.115	106	2.149	0.195	0.317	3.761	18.298
4	108	2.575	110	1.826	0.381	0.280	3.176	15.289
5	110	2.333	102	0.972	0.232	0.149	4.753	22.003
6	108	1.872	103	2.214	0.158	0.217	3.907	17.928
7	111	3.957	106	2.240	0.103	0.150	4.477	22.079
8	107	2.866	105	1.270	0.257	0.186	3.807	16.939
9	111	2.939	108	1.037	0.373	0.285	3.142	14.970
10	112	2.187	106	1.115	0.126	0.189	4.137	20.491
100	114	4.151	107	1.774	0.091	0.112	4.800	23.608

where w_t represents the tth quality characteristic weight, n is the number of objectives, and $\varphi\left(x_r^*, x_i^*\right)$ is the value of GRG.

In GRA, GRG is adopted to determine the relationship between the comparable sequence and the reference sequence. The weights of objectives are different in this study. Therefore, (17) is adopted to calculate the GRG. The traditional CV method, which is simple and convenient, has a firm mathematical theory foundation and high precision. Noteworthily, the average value of the certain original sequence is so small that a slight disturbance can make a huge impact and lead to the result of CV becomes imprecise and even erroneous. The traditional CV cannot be applied to lightweight optimization of the passenger car seat frame because values in the strain index sequence have wide rangeability while the average value of the strain index sequence is much less than 1 in the seat performance objectives. Accordingly, in order to obtain accurate weight coefficients, the original sequences need to be normalized, and the coefficient of variation can be obtained by different formulas. In this paper, the optimized coefficient of variation method is innovated and applied to determine the corresponding weight of objective characteristics in each safety test.

6.2 Coefficient of variation method and optimized coefficient of variation method

The coefficient of variation method directly uses the information contained in each target to calculate the weight of the criteria. The coefficient of variation method is applied to determine the contribution values of the sequences on the basis of the degree of dispersion. The influence of different dimensions is eliminated by the variable coefficient. The weight of variation coefficient can be obtained by firstly calculating the absolute and relative variation degree of each original sequence, then computing the variation coefficient, and normalizing it. The corresponding calculation process is as follows (Garg and Pachori (2019), Li et al. (2019):

Step 1. Obtain the average value $\overline{a_t}$ of the tth sequence:

$$\overline{a_t} = \frac{1}{K}\sum_{k=1}^{K} a_{tk} \tag{18}$$

Table 14 SAT results of grey relational generation

No.	SI_{B1}	SA_1/mm	G/kg	Cost/¥
Idea	1.000	1.000	1.000	1.000
1	1.000	1.000	0.000	0.000
2	0.339	0.766	0.273	0.489
3	0.780	0.909	0.363	0.392
4	0.437	0.551	0.545	0.668
15	0.462	0.815	0.636	0.588

Table 15 SBST results of grey relational generation

No.	SI_{B2}	SD_1/mm	G/kg	Cost/¥
Idea	1.000	1.000	1.000	1.000
1	0.987	0.903	0.647	0.529
2	0.537	0.823	0.765	0.835
3	0.776	0.869	0.824	0.793
4	0.977	0.904	0.295	0.305
25	0.109	0.773	1.000	1.000

Table 16 HSST results of grey relational generation

No.	SI_{B3}	SL_1/mm	G/kg	Cost/¥
Idea	1.000	1.000	1.000	1.000
1	0.245	0.000	0.739	0.834
2	0.440	0.976	0.348	0.423
3	0.425	0.983	0.174	0.350
4	0.520	0.946	0.435	0.428
25	0.000	0.444	1.000	1.000

Step 2. Obtain the standard deviation D_t of the tth sequence:

$$\mathrm{D}_t = \sqrt{\frac{1}{K}\sum_{K=1}^{K}\left(a_t - \overline{a_t}\right)^2} \tag{19}$$

Step 3. Obtain the coefficient of variation δ_t of the tth sequence:

$$\delta_t = \frac{D_t}{\overline{a_t}} \tag{20}$$

Step 4. Obtain the weight w_t of the tth sequence:

$$w_t = \frac{\delta_t}{\sum_{i=1}^{n}\delta_t} \tag{22}$$

The calculation process of optimized coefficient of variation is as follows:

Table 17 FULT results of grey relational generation

No.	SI_{B1}	SA_1/mm	G/kg	Cost/¥
Idea	1.000	1.000	1.000	1.000
1	0.885	0.903	0.588	0.647
2	0.000	0.000	0.235	0.505
3	0.389	0.745	1.000	1.000
4	0.968	0.981	0.118	0.263
25	0.242	0.631	0.882	0.926

Table 18 APT results of grey relational generation

No.	SA_1/mm	G/kg	Cost/¥
Idea	1.000	1.000	1.000
1	0.876	0.000	0.032
2	0.433	0.684	0.654
3	0.823	0.334	0.207
4	0.619	0.003	0.139
40	0.640	0.200	0.372

Step 1. Normalize the original sequences according to their characteristics. The original sequence with the characteristic of "the smaller, the better" can be normalized by (9); the original sequence with the characteristic of "the larger, the better" can be normalized by (10); the optimal value of the original sequence can be normalized by (11) when equals to the target value.

Step 2. Obtain the average value $\overline{a_t}$ of the tth sequence:

$$\overline{a_t} = \frac{1}{K}\sum_{k=1}^{K} a_{tk} \tag{18}$$

Step 3. Obtain the standard deviation D_t of the tth sequence:

$$\mathrm{D}_t = \sqrt{\frac{1}{K}\sum_{K=1}^{K}\left(a_t - \overline{a_t}\right)^2} \tag{19}$$

Table 19 50 DF/RCPT results of grey generation

No.	FC-$SI_{Bi...Bj}$	RC-$SI_{Bi...Bj}$	G/kg	Cost/¥
Idea	1.000	1.000	1.000	1.000
1	0.770	0.727	0.706	0.739
2	0.426	0.452	0.871	0.896
3	0.695	0.106	0.849	0.840
4	0.238	0.251	0.940	0.937
5	0.604	0.761	0.695	0.720
6	0.786	0.496	0.826	0.852
7	0.920	0.758	0.738	0.718
8	0.542	0.617	0.842	0.884
9	0.257	0.232	0.945	0.947
10	0.865	0.605	0.790	0.769
100	0.950	0.906	0.687	0.669

Table 20 Optimized coefficient of variation weights of L-optimization

Performance quotas	SI_{Bi}	Displacement (mm)	G/kg	Cost/¥
SAT	0.2417	0.1863	0.3135	0.2585
SBST	0.2402	0.1375	0.3128	0.3095
HSST	0.3135	0.1287	0.2941	0.2637
FULT	0.2148	0.1679	0.3368	0.2805
APT	•	0.3917	0.2892	0.3191

Step 4. If the ratio of the maximum to the minimum for a certain original sequence is larger than 10 times, or the value of the maximum minus the minimum for original sequence of strain index is bigger than 0.5,[5] the coefficient of variation $\delta_t$of the all sequences may be obtained as below:

$$\delta_t = \frac{D_t}{\overline{a_t}} \tag{20}$$

If the ratio of the maximum to the minimum for a certain original sequence is smaller than 10 times, or the value of the maximum minus the minimum for original sequence of strain index is smaller than 0.5, the coefficient of variation $\delta_t$of the all sequences may be obtained as below:

$$\delta_t = \frac{\overline{a_t}}{D_t} \tag{21}$$

Step 5. Obtain the weight w_t of the tth sequence:

$$w_t = \frac{\delta_t}{\sum_{i=1}^{n} \delta_t} \tag{22}$$

where K denotes the amount of data in a certain sequence, tth is the code of the each sequence, $\overline{a_t}$ is the average value of the tth sequence, a_{tk} is the kth value of the tth sequence and $k = 1,2,3...K$, D_t is the standard deviation of the tth sequence , $\delta_t$is the coefficient of variation of the tth sequence, and w_t is the weight of the tth sequence.

Table 21 Optimized coefficient of variation weights of G-optimization

Performance quotas	FC-$SI_{Bi...Bj}$	RC-$SI_{Bi...Bj}$	G/kg	Cost/¥
50 DF/RCPT	0.1581	0.1347	0.3515	0.3557

[5] The value of 10 times 0.5 represents experimental thresholds.

Table 22 SAT grey relational coefficient and grey relational grade of GRA&OCV

No.	Grey relational coefficient				Grey relational order grade	
	SI_{B1}	SA_1/mm	G/kg	Cost/¥		
Idea	1.000	1.000	1.000	1.000		
1	1.000	1.000	0.333	0.333	0.619	3
2	0.431	0.681	0.407	0.494	0.487	11
3	0.694	0.846	0.440	0.451	0.580	5
4	0.470	0.527	0.524	0.601	0.531	7
14	0.419	0.474	1.000	1.000	0.761	1
15	0.482	0.730	0.579	0.548	0.576	6

The optimized coefficient of variation method is different from coefficient of variation. In the CV, the original sequences can be used directly, while the original sequences need to be normalized in the OCV. After the original sequence is normalized, formulas (18), (19), (20), and (22) are adopted to calculate the weights of different objectives in SAT, SBST, and FULT; and formula (18), (19), (20), (22) are adopted in APT and 50 DF/RCPT.

6.3 Lightweight optimization results

As shown in Tables 20 and 21, the results calculated by the OCV method are the weights of each safety test in this paper. Also, the grey relational grade can be obtained by (17).

The GRG is the degree of relationship between the comparability sequence and the reference sequence, and the reference sequence denotes the best performance. Therefore, the comparability sequence with higher GRG is closer to the optimal value. As shown in Tables 22, 23, 24, 25, 26, and 27, the values of GRG calculated for each experiment are arranged from big to small and listed on the right side of these tables, while the No. 14, No. 25, No. 25, No. 3, No. 26, and No. 34 correspondently show the biggest GRG. Finally, in SAT, SBST, HSST, FULT, APT, and 50 DF/RCPT, the No.14,

Table 23 SBST grey relational coefficient and grey relational grade of GRA&OCV

No.	Grey relational coefficient				Grey relational order grade	
	SI_{B2}	SD_1/mm	G/kg	Cost/¥		
Idea	1.000	1.000	1.000	1.000		
1	0.975	0.837	0.586	0.515	0.692	3
2	0.519	0.739	0.680	0.752	0.672	4
3	0.691	0.792	0.740	0.707	0.725	2
4	0.956	0.839	0.415	0.418	0.604	10
25	0.359	0.688	1.000	1.000	0.803	1

Table 24 HSST grey relational coefficient and grey relational grade of GRA&OCV

No.	Grey relational coefficient				Grey relational order grade	
	SI_{B3}	SL_1/mm	G/kg	Cost/¥		
Idea	1.000	1.000	1.000	1.000		
1	0.398	0.333	0.657	0.751	0.559	10
2	0.472	0.955	0.434	0.464	0.521	15
3	0.465	0.966	0.377	0.435	0.496	18
4	0.510	0.903	0.469	0.467	0.537	13
25	0.333	0.473	1.000	1.000	0.723	1

No. 25, No. 25, No. 3, No. 26, and No. 34 experiment respectively reach the best scheme in which the thicknesses of the parts are dealt with by the rounding-off method in Table 28.

7 Comparison and verification

In order to assess the proposed method of GRA&OCV in this study, a comprehensive comparison among the results from original design, GRA&OCV, GRA&CV, TOPSIS&OCV, and TOPSIS&CV is conducted. We introduce TOPSIS with different weighting arrangement strategies because this is a classical method for solving multi-attribute decision problems (Nguyen et al. (2014); Wang et al. (2016); Xiong et al. (2018a, b). In this study, the weights of CV and OCV are selected to apply in TOPSIS.

Tables 29 and 30 are the weights obtained by the CV. Similar to GRA&OCV, the results obtained from GRA&CV, TOPSIS&CV, and TOPSIS&OCV are demonstrated in SAT, SBST, HSST, FULT, APT, and 50 DF/RCPT. The best compromise between material and thickness for GRA&CV, TOPSIS&CV, and TOPSIS&OCV are shown in Tables 31, 32, and 33.

By comparing the results among GRA&OCV (Table 28), GRA&CV (Table 31), TOPSIS&CV (Table 32), and TOPSIS&OCV (Table 33), we notice that apart from the same results with safety test APT, the best compromise schemes from other safety tests are different. In order to have a deeper comparison and explore the advantages and disadvantages of the four methods, in this paper, the vibrational and safety performance models of the passenger car seat according to the compromise combination scheme of material thickness in four different methods are reconstructed, and then these models will be simulated in all safety tests.

Table 25 FULT grey relational coefficient and grey relational grade of GRA&OCV

No.	Grey relational coefficient				Grey relational order grade	
	SI_{B4}	SO_1/mm	G/kg	Cost/¥		
Idea	1.000	1.000	1.000	1.000		
1	0.814	0.837	0.548	0.586	0.664	4
2	0.333	0.333	0.395	0.502	0.402	13
3	0.450	0.662	1.000	1.000	0.825	1
4	0.940	0.964	0.362	0.404	0.599	8
25	0.397	0.575	0.810	0.871	0.699	3

Table 26 APT grey relational coefficient and grey relational grade of GRA&OCV

No.	Grey relational coefficient			Grey relational order grade	
	SR_1/mm	G/kg	Cost/¥		
Idea	1.000	1.000	1.000		
1	0.801	0.333	0.341	0.519	20
2	0.469	0.613	0.591	0.549	17
3	0.737	0.429	0.387	0.536	19
4	0.568	0.334	0.367	0.622	6
26	0.423	0.997	1.000	0.773	1
40	0.581	0.385	0.443	0.480	22

As shown in Tables 35 and 36, the results of the lightweight objectives are compared among the original design and the best scheme obtained by the GRA&OCV, GRA&CV, TOPSIS&CV, and TOPSIS&OCV. The explanations of column and row heading for Tables 35 and 36 are shown in Table 34. In addition, to compare the performance of the best scheme obtained by GRA&OCV, GRA&CV, TOPSIS&CV, TOPSIS&OCV, and the original design in detail, the strain index of each optimization component and displacement of each key measurement point are selected for comparison.

In Tables 35 and 36, the results of the original design are lower than international standard, since the SI_{B4} in the FULT and the SI_{B5} in the 50 DRCPT are both larger than 1 and the SR_1 in the APT is larger than 130 mm. However, the best schemes obtained by GRA&OCV, GRA&CV, TOPSIS&CV, and TOPSIS&OCV can meet the design requirements[6] of passenger car seat. In the best schemes, the masses optimized by GRA&OCV, GRA&CV, TOPSIS&CV, and TOPSIS&OCV are respectively reduced by 2.08 kg, −1.24 kg, −0.32 kg, and 1.16 kg, namely, the relative ratios of lightweight are respectively 12.46%, −7.43%, −1.92%, and 6.95%. The total material costs are respectively decreased by ¥7.72, ¥-8.97, ¥-4.3, and ¥3.48, namely, the relatively price-decrease ratios are 17.00%, −19.75%, −9.47%, and 7.66%. It can be seen that the best

[6] The design requirements, which are more strict than international safety standards, are proposed by a corporative company in China.

Table 27 50 DF/RCPT grey relational coefficient and grey relational grade of GRA&OCV

No.	Grey relational coefficient				Grey relational order grade	
	FC-$SI_{Bi...Bj}$	RC-$SI_{Bi...Bj}$	G/kg	Cost/¥		
Idea	1.000	1.000	1.000	1.000		
1	0.685	0.647	0.630	0.657	0.650	85
2	0.465	0.477	0.795	0.828	0.712	31
3	0.621	0.359	0.768	0.757	0.686	59
4	0.396	0.400	0.892	0.888	0.746	10
5	0.558	0.676	0.621	0.641	0.626	88
6	0.700	0.498	0.742	0.771	0.713	28
7	0.862	0.674	0.656	0.639	0.685	60
8	0.522	0.566	0.760	0.811	0.714	25
9	0.402	0.394	0.901	0.904	0.755	6
10	0.788	0.559	0.705	0.684	0.691	50
34	0.561	0.333	1.000	1.000	0.841	1
100	0.910	0.841	0.615	0.601	0.687	55

Table 28 The best compromise results of safety tests of GRA&OCV

Performance quotas	Optimization parts	Material	Thickness	Optimization thickness
SAT	B1	114	1.311	1.3
SBST	B2	112	1.000	1.0
HSST	B3	106	0.950	1.0
FULT	B4	111	0.999	1.0
APT	B5	104	0.529	0.5
	B6	112	1.188	1.2
50 DF/RCPT	B7	106	2.067	2.0
	B8	114	1.327	1.3
	B9	107	2.867	2.9
	B10	110	0.803	0.8
	B11	104	1.244	1.2

scheme obtained by GRA&OCV has more obvious lightweight effect and its price is lower than original design, GRA&CV, TOPSIS&CV, and TOPSIS&OCV. Meanwhile, the first-order vibrational frequencies in the best scheme by original design, GRA&OCV, GRA&CV, TOPSIS&CV, and TOPSIS&OCV are respectively 27.75 Hz, 24.79 Hz, 25.77 Hz, 28.58 Hz, and 26.00 Hz. The first-order vibrational frequencies ranking (high to low) of seat with different methods is TOPSIS&CV, original design, TOPSIS&OCV, GRA&CV, and GRA&OCV; in these schemes, the first-order vibrational frequencies are all higher than 18 H_Z and thus meet the design requirements. In terms of performance parameters, each key point displacement and strain index of the best scheme by GRA&OCV is smaller than the original design and meets the design threshold. Each key point

Table 29 Coefficient of variation weights of L-optimization

Performance quotas	SI_{Bi}	Displacement/mm	G/kg	Cost/¥
SAT	0.3071	0.3090	0.2003	0.1836
SBST	0.7803	0.0398	0.0896	0.0903
HSST	0.4831	0.1897	0.1623	0.1649
FULT	0.7013	0.1362	0.0847	0.0778
APT	•	0.0994	0.4476	0.4530

Table 30 Coefficient of variation weights of G-optimization

Performance quotas	FC-$SI_{Bi...Bj}$	RC-$SI_{Bi...Bj}$	G/kg	Cost/¥
50 DF/RCPT	0.4079	0.2467	0.1756	0.1698

Table 31 The best compromise results of safety tests of GRA&CV

Performance quotas	Optimization parts	Material	Thickness	Optimization thickness
SAT	B1	113	2.160	2.2
SBST	B2	113	1.240	1.2
HSST	B3	109	1.500	1.5
FULT	B4	109	1.640	1.6
APT	B5	104	0.529	0.5
	B6	112	1.188	1.2
50 DF/RCPT	B7	109	4.103	4.1
	B8	111	2.185	1.0
	B9	109	3.740	2.1
	B10	111	0.480	0.8
	B11	107	2.059	1.9

Table 33 The best compromise results of safety tests of TOPSIS&OCV

Performance quotas	Optimization parts	Material	Thickness	Optimization thickness
SAT	B1	113	1.543	1.5
SBST	B2	113	1.240	1.2
HSST	B3	109	1.500	1.5
FULT	B4	110	1.200	1.2
APT	B5	104	0.529	0.5
	B6	112	1.188	1.2
50 DF/RCPT	B7	114	1.970	2.0
	B8	110	1.531	1.5
	B9	109	2.358	2.4
	B10	109	0.603	0.6
	B11	104	2.980	3.0

displacement and strain index of the best scheme by original design, GRA&CV, TOPSIS&CV, and TOPSIS&OCV is much less than the original design. Meanwhile, the design margin is too large.

Noteworthily, the GRA is very straightforward in prioritizing alternatives and calculation. Besides, the GRA can deal with multi-objective optimization problems flexibly. For example, in the GRA, the original sequences can be normalized to different comparable sequences based on corresponding characteristics, which will lead to different results. Furthermore, the distinguishing coefficient ω can be adjusted based on practical situation, and different distinguishing coefficients can lead to different results. Moreover, w.r.t. computation efficiency, and application range, GRA is superior to many other multi-criterial decision-making methods including TOPSIS (Wang et al. (2013). Through comparing the weights obtained by the optimized coefficient of variation method and the coefficient of variation method, it can be seen that the OCV assigns more weights to the total mass and total material cost of the components, while CV assigns more weights to the performance objectives such as strain index and key point displacement. Therefore, GRA&CV and TOPSIS&CV tend to obtain better performance, while GRA&OCV and TOPSIS&OCV are more likely to obtain smaller total mass and material costs when adopted in the multi-objective lightweight design of the passenger car seat. However, the scheme obtained by GRA&OCV has smaller mass and costs when compared with TOPSIS&OCV. Actually, excessive design margin for performances of passenger car seat may increase

Table 32 The best compromise results of safety tests of TOPSIS&CV

Performance quotas	Optimization parts	Material	Thickness	Optimization thickness
SAT	B1	113	1.851	1.9
SBST	B2	113	1.240	1.2
HSST	B3	109	1.500	1.5
FULT	B4	110	1.400	1.4
APT	B5	104	0.529	0.5
	B6	112	1.188	1.2
50 DF/RCPT	B7	109	2.358	2.4
	B8	112	1.924	1.9
	B9	112	4.055	4.1
	B10	109	0.642	0.6
	B11	103	1.865	1.9

Table 34 The explanation of column and row heading for Tables 35 and 36

Column	Explanation
Type	The kind of safety tests for the passenger car seat
Objects/parts	The opti-components correspondingly for the passenger car seat in safety tests
Original	The original simulation results
GRA&OCV	The simulation results of the best scheme obtained by the grey relational analysis and optimized coefficient of variation
GRA&CV	The simulation results of the best scheme obtained by the grey relational analysis and coefficient of variation
TOPSIS&CV	The simulation results of the best scheme obtained by the TOPSIS and coefficient of variation
TOPSIS&OCV	The simulation results of the best scheme obtained by the TOPSIS and optimized coefficient of variation
Error (%)	The relative deviation between the corresponding lightweight scheme and the original design
SPI	The empirical reference standard for each seat safety test

Table 35 Lightweight comparison results

Type	Objects/parts	Quotas	Original	GRA&OCV	Error (%)	GRA&CV	Error (%)	SPI
Lightweight criteria	Seat frame	G/kg	16.69	14.61	−12.46	17.93	7.43	●
Cost	Optimized parts	Cost/¥	45.41	37.69	−17.00	54.38	19.75	●
Vibrational criteria	Seat frame	F_1/H_Z	27.75	24.79	−10.67	25.77	−7.14	≥18
		F_2/H_Z	35.67	32.24	−9.62	33.86	−5.07	●
		F_3/H_Z	42.35	38.73	−8.55	42.28	−0.17	●
SAT	B1	SA_1/mm	31.98	40.55	26.80	20.71	−35.24	●
		SI_{B1}	0.66	0.72	9.09	0.27	−59.09	≤0.95
SBST	B2	SD_1/mm	201.65	172.73	−14.34	43.99	−78.18	●
		SI_{B2}	0.25	0.84	236.00	0.00	−100.00	≤0.95
HSST	B3	SL_1/mm	62.45	61.42	−1.65	58.63	−6.12	≤82
		SI_{B3}	0.61	0.94	54.10	0.01	−98.36	≤0.95
FULT	B4	SO_1/mm	120.00	79.72	−33.57	63.12	−47.40	≤150
		SI_{B4}	1.07	0.55	−48.60	0.47	−56.07	≤0.95
APT	B5 B6	SR_1/mm	137.44	118.62	−13.69	109.65	−20.22	≤130
50 DFCPT	B1	SI_{B1}	0.11	0.57	418.18	0.03	−72.73	≤0.95
	B2	SI_{B2}	0.06	0.08	33.33	0.04	−33.33	≤0.95
	B3	SI_{B3}	0.00	0.00	0.00	0.00	0.00	≤0.95
	B4	SI_{B4}	0.01	0.00	−100.00	0.00	−100.00	≤0.95
	B5	SI_{B5}	0.26	0.43	65.38	0.35	34.62	≤0.95
	B6	SI_{B6}	0.06	0.05	−16.67	0.10	66.67	≤0.95
	B7	SI_{B7}	0.04	0.07	75.00	0.04	0.00	≤0.95
	B8	SI_{B8}	0.17	0.31	82.35	0.14	−17.65	≤0.95
	B9	SI_{B9}	0.21	0.21	0.00	0.23	9.52	≤0.95
	B10	SI_{B10}	0.15	0.32	113.33	0.18	20.00	≤0.95
	B11	SI_{B11}	0.06	0.32	433.33	0.04	−33.33	≤0.95
50 DRCPT	B1	SI_{B1}	0.11	0.17	54.55	0.02	−81.82	≤0.95
	B2	SI_{B2}	0.23	0.20	−13.04	0.23	0.00	≤0.95
	B3	SI_{B3}	0.37	0.36	−2.70	0.10	−72.97	≤0.95
	B4	SI_{B4}	0.09	0.03	−66.67	0.09	0.00	≤0.95
	B5	SI_{B5}	1.21	0.89	−26.45	0.93	−23.14	≤0.95
	B6	SI_{B6}	0.01	0.00	−100.00	0.00	−100.00	≤0.95
	B7	SI_{B7}	0.10	0.80	700.00	0.14	40.00	≤0.95
	B8	SI_{B8}	0.20	0.35	75.00	0.10	−50.00	≤0.95
	B9	Si_{B9}	0.26	0.19	−26.92	0.11	−57.69	≤0.95
	B10	Si_{B10}	0.12	0.17	41.67	0.28	133.33	≤0.95
	B11	Si_{B11}	0.18	0.27	50.00	0.07	−61.11	≤0.95

total mass and total cost in the vein. In conclusion, the best scheme obtained by GRA&OCV, which is more in line with the requirements of seat lightweight design, is better.

8 The methods of safety tests

The test methods of each safety test for passenger car seat are as follows:

① Seatbelt Anchorage Test (SAT):

- A complete and fully trimmed seat assembly should be fitted to a fixture which can simulate the body shell. The squab should be set in the nominal design position (25° or other specified).
- The simulated ribbon was used to apply 13,500 N ± 200 N test load to the dummy's upper body module in the direction of 10° along the horizontal line.
- The test load of 13,500 N ± 200 N was applied to the lower body module in the direction of 10° upward along the horizontal line; apply a force equal to 20 times the mass of the seat assembly along the horizontal line.

Table 36 Lightweight comparison results

Type	Objects/parts	Quotas	Original	TOPSIS&CV	Error (%)	TOPSIS&OCV	Error (%)	SPI
Lightweight criteria	Seat frame	G/kg	16.69	17.01	1.92	15.53	−6.95	●
Cost	Optimized parts	Cost/¥	45.41	49.71	9.47	41.93	−7.66	●
Vibrational criteria	Seat frame	F_1/H_Z	27.75	28.58	2.99	26.00	−6.31	≥18
		F_2/H_Z	35.67	38.62	8.27	32.31	−9.42	●
		F_3/H_Z	42.35	43.53	2.79	39.40	−6.97	●
SAT	B1	SA_1/mm	31.98	21.07	−34.12	33.32	4.19	●
		SI_{B1}	0.66	0.37	−43.94	0.41	−37.88	≤0.95
SBST	B2	SD_1/mm	201.65	167.68	−16.85	168.47	−16.45	●
		SI_{B2}	0.25	0.00	−100.00	0.00	−100.00	≤0.95
HSST	B3	SL_1/mm	62.45	38.90	−37.71	39.17	−37.28	≤82
		SI_{B3}	0.61	0.01	−98.36	0.01	−98.36	≤0.95
FULT	B4	SO_1/mm	120.00	65.36	−45.53	69.28	−42.27	≤150
		SI_{B4}	1.07	0.02	−98.13	0.03	−97.20	≤0.95
APT	B5 B6	SR_1/mm	137.44	118.35	−13.89	119.13	−13.32	≤130
50 DFCPT	B1	SI_{B1}	0.11	0.01	−90.91	0.01	−90.91	≤0.95
	B2	SI_{B2}	0.06	0.05	−16.67	0.07	16.67	≤0.95
	B3	SI_{B3}	0.00	0.00	0.00	0.00	0.00	≤0.95
	B4	SI_{B4}	0.01	0.00	−100.00	0.00	−100.00	≤0.95
	B5	SI_{B5}	0.26	0.37	42.31	0.39	50.00	≤0.95
	B6	SI_{B6}	0.06	0.10	66.67	0.10	66.67	≤0.95
	B7	SI_{B7}	0.04	0.02	−50.00	0.21	425.00	≤0.95
	B8	SI_{B8}	0.17	0.15	−11.76	0.13	−23.53	≤0.95
	B9	SI_{B9}	0.21	0.14	−33.33	0.21	0.00	≤0.95
	B10	SI_{B10}	0.15	0.10	−33.33	0.31	106.67	≤0.95
	B11	SI_{B11}	0.06	0.13	116.67	0.11	83.33	≤0.95
50 DRCPT	B1	SI_{B1}	0.11	0.02	−81.82	0.04	−63.64	≤0.95
	B2	SI_{B2}	0.23	0.24	4.35	0.24	4.35	≤0.95
	B3	SI_{B3}	0.37	0.32	−13.51	0.31	−16.22	≤0.95
	B4	SI_{B4}	0.09	0.03	−66.67	0.05	−44.44	≤0.95
	B5	SI_{B5}	1.21	0.83	−31.40	0.94	−22.31	≤0.95
	B6	SI_{B6}	0.01	0.00	−100.00	0.00	−100.00	≤0.95
	B7	SI_{B7}	0.10	0.09	10.00	0.65	550.00	≤0.95
	B8	SI_{B8}	0.20	0.11	−45.00	0.31	55.00	≤0.95
	B9	Si_{B9}	0.26	0.08	−69.23	0.13	−50.00	≤0.95
	B10	Si_{B10}	0.12	0.18	50.00	0.20	66.67	≤0.95
	B11	Si_{B11}	0.18	0.05	−72.22	0.15	−16.67	≤0.95

- During the test, all components of the seat frame should not fail.

② Seat Back Strength Test (SBST):

- A complete and fully trimmed seat assembly should be fitted to a fixture which can simulate the body shell. The squab should be set in the nominal design position.
- A force producing a moment of 635 Nm in relation to the H-point should be used rearward to the upper part of the seat back frame by a manikin back form, keep as 10 s, continue loading to 1500 Nm, and maintain 10 s.
- During the test, all components of the seat frame should not fail.

③ Headrest Static Strength Test (HSST):

- A complete and fully trimmed front seat assembly should be fitted to a rigid fixture. The displaced reference line r_1 should be determined through using

the manikin back form an initial force producing a rearward moment of 373 Nm about the H-point.
- By means of a spherical head form of 165 mm diameter, an initial force producing a moment of 373 Nm about the H-point should be used at a point 65 mm below the top of the head restraint.
- The force should be used at right angles to the displaced reference line r_1, while the back form is retained in its displaced position r_1, and the head restraint and its anchorage should be such that the maximum backward displacement X of the head form should be less than 82 mm.
- After the above requirements have been fulfilled, the force applied to the head form should be increased to 1070 N or until the seat back breaks.
- The head restraint and its anchorages should withstand the increased force without failure.

④ Frame Ultimate Load Test (FULT):

- Set the seat to a rig representing the vehicle floor mounting condition. The seat squab should be set to 25° rearward from the vertical unless otherwise specified.
- Set the seat on its highest position unless otherwise specified. Apply a torque of 2500 Nm to seat frame about the recline mechanism pivot center.
- During the test, the deflection, measured along the line of the action of the force, should be less than 150 mm under a torque of 1500 Nm.
- At the end of the test, both seat structures must be free from cracks or broken fixings.

⑤ Antisubmarine Pan Test (APT):

- Application force to the seat cushion is by the SAE buttocks, and the force point in the vertical plane cushion 120-mm H-point forward and the direction Z-angle 20° ~ 35° in the overall vehicle coordinate system, preload 100 N and fully release the applied force by 2 cycles restart to apply the force to 100 N and start to record, loading speed 150 mm/min, up until the static force to 15,000 N.
- The recorded curve should be to the left of the standard datum line, and the displacement should be 130 mm when the force is 15,000 N, while the standard requires the test curve to be to the left of the standard datum line.
- Therefore, if the displacement is less than 130 mm when the force is applied to 15,000 N, it should be considered qualified; otherwise the test should not pass.

⑥ 50 Dummy Frontal Crash Performance Test (50 DFCPT):

- Fit a fully trimmed seat assembly to a body shell or alternatively to a representative fixture. And fit the body shell or fixture to the sled test facility. Set the seat squab at the design angle. Set the height adjuster, slides, and head restraint to mid-positions for the 50th%ile Hybrid III dummy.
- Apply a frontal longitudinal deceleration equivalent to the vehicle's 56.327 km/h crash pulse. The seat's antisubmarine panel and other components such as seat belt anchors are expected to have deformed in the impact, but deformation must not be so excessive as to allow manikin excursion.
- There must be no evidence of breaking, tearing, or other structural collapses.

⑦ 50 Dummy Rearal Crash Performance Test (50 DRCPT):

- Fit a fully trimmed seat assembly to a body shell or alternatively to a representative fixture. And then fit the body or fixture to the sled test facility. Set the seat squab at the design angle. Set the height adjuster, slides, and head restraint to positions appropriate for the 50th%ile Hybrid III dummy in use.
- Apply a rearward longitudinal deceleration equivalent to the vehicle's 48.28-km/h crash pulse.
- There must be no evidence of breaking, tearing, or other structural collapses.

9 Conclusion

In this paper, a detailed optimization design method and a design process are proposed in lightweight optimization for passenger car seat to assess the effectiveness of the lightweight design. In more detail, the material thickness FEA models, the optimal latin hypercube sampling method, the ratio of energy absorption to mass method, and the grey relational analysis and optimized coefficient of variation are simultaneously applied to the passenger car seat frame for multi-objective lightweight optimization. On the basis of the achieved results, the following consequences can be drawn:

(1). The method of ratio of energy absorption to mass, which is adopted to select the lightweight opti-components, is simple and effective because of the few and symmetrically distributed components of passenger car seat frame.
(2). In the L-optimization, the strain index of components, the displacement of key measurement points, and the total mass and material cost of the opti-components are regarded as the four optimization objectives. In the G-

optimization, the strain index of components and the total mass and material cost of the opti-components are regarded as the three optimization objectives. The optimum material thickness combination scheme of opti-components can be acquired by GRA&OCV.

(3). According to the comparisons and verifications of the best schemes among the GRA&OCV, the TOPSIS&OCV, the GRA&CV, and the TOPSIS&CV, it can be seen that the OCV assigns more weights to the total mass and total material cost of the components, while the CV assign more weights to the safety performance. Moreover, both of the schemes from the GRA&OCV and TOPSIS&OCV met the design requirement, but the result of best scheme obtained by GRA&OCV is lighter. Hence, the GRA&OCV applied to the multi-objective lightweight optimization of passenger car seat is better and more suitable to the seat lightweight design requirements.

(4). The conclusions present that, by the GRA&OCV, the total material cost of the opti-components can be reduced by ¥7.72 (17.00%) and the total mass of the passenger car seat frame can be reduced by 2.08 kg (12.46%), while the safety and the vibrational performance of the passenger car seat are well guaranteed and meet the design requirements. Therefore, the GRA&OCV can be efficaciously applied to multi-objective lightweight optimization of the passenger car seat frame.

Acknowledgments The authors would like to express their gratitude to the Wenzhou University.

Funding information The research work was financially supported by the National Natural Science Foundation of China (Grant No.51905383 and 51475336).

Compliance with ethical standards

Conflict of interest The authors declare that they have no conflict of interest.

Replication of results Original data are provided in the supplementary material.

References

Alharbi S, Raun WR, Arnall DB, Zhang HL (2019) Prediction of maize (Zea mays L.) population using normalized-difference vegetative index (NDVI) and coefficient of variation (CV). J Plant Nutr 42: 673–679. https://doi.org/10.1080/01904167.2019.1568465

Barán B, Laufer M (2015) Generalization of the MOACS algorithm for many objectives: an application to motorcycle distribution. CLEI Electron J 18:9–9

Baynal K, Sari T, Akpinar B (2018) Risk management in automotive manufacturing process based on FMEA and grey relational analysis: a case study. Adv Prod Eng Manag 13:69–80. https://doi.org/10.14743/apem2018.1.274

Cai KF, Wang DF (2017) Optimizing the design of automotive S-rail using grey relational analysis coupled with grey entropy measurement to improve crashworthiness. Struct Multidiscip Optim 56: 1539–1553. https://doi.org/10.1007/s00158-017-1728-y

Chau NL, Le HG, Dao TP, Dang VA (2019) Design and Optimization for a New Compliant Planar Spring of Upper Limb Assistive Device Using Hybrid Approach of RSM-FEM and MOGA. Arab J Sci Eng 44:7441–7456. https://doi.org/10.1007/s13369-019-03795-w

Chen CH (2019) A new multi-criteria assessment model combining GRA techniques with intuitionistic fuzzy entropy-based TOPSIS method for sustainable building materials supplier selection. Sustainability 11:18. https://doi.org/10.3390/su11082265

Chen W, Zuo W (2014) Component sensitivity analysis of conceptual vehicle body for lightweight design under static and dynamic stiffness demands. Int J Veh Des 66(2):107–123

Choi BC, Cho S, Kim CW (2018) Kriging model based optimization of MacPherson strut suspension for minimizing side load using flexible multi-body dynamics. Int J Precis Eng Manuf 19:873–879. https://doi.org/10.1007/s12541-018-0103-2

Deng J (1982) Control problems of grey systems. Syst Control Lett 1: 288–294

Deng J (1989) Introduction to grey system theory. The Journal of grey system 1(1):1–24

Duan LB, Jiang HB, Cheng AG, Xue HT, Geng GQ (2019) Multi-objective reliability-based design optimization for the VRB-VCS FLB under front-impact collision. Struct Multidiscip Optim 59: 1835–1851. https://doi.org/10.1007/s00158-018-2142-9

Fang JG, Gao YK, Sun GY, Xu CM, Li Q (2015) Multiobjective robust design optimization of fatigue life for a truck cab. Reliab Eng Syst Saf 135:1–8. https://doi.org/10.1016/j.ress.2014.10.007

Fang J, Sun G, Qiu N et al (2017) On design optimization for structural crashworthiness and its state of the art. Struct Multidiscip Optim 55: 1091–1119. https://doi.org/10.1007/s00158-016-1579-y

Fossati GG, Miguel LFF, Casas WJP (2019) Multi-objective optimization of the suspension system parameters of a full vehicle model. Optim Eng 20:151–177. https://doi.org/10.1007/s11081-018-9403-8

Gao DW, Li XY, Chen HF (2019) Application of improved particle swarm optimization in vehicle crashworthiness. Math Probl Eng 10. https://doi.org/10.1155/2019/8164609

Garg N, Pachori M (2019) Use of coefficient of variation in calibration estimation of population mean in stratified sampling. Commun Stat-Theory Methods 11. https://doi.org/10.1080/03610926.2019.1622729

Golbabaie F, Omidvar M, Nirumand F (2019) Risk assessment of heat stress using the AHP and TOPSIS methods in fuzzy environment- a case study in a foundry shop. J Health Saf Work 8:397–+

Gu XG, Sun GY, Li GY, Mao LC, Li Q (2013) A Comparative study on multiobjective reliable and robust optimization for crashworthiness design of vehicle structure. Struct Multidiscip Optim 48:669–684. https://doi.org/10.1007/s00158-013-0921-x

Han HZ, Yu RT, Li BX, Zhang YN (2019) Multi-objective optimization of corrugated tube inserted with multi-channel twisted tape using RSM and NSGA-II. Appl Therm Eng 159:13. https://doi.org/10.1016/j.applthermaleng.2019.113731

Kim KS, Cho HS, Kim YC, Cho JU (2014) Structural study of automotive seat frame with high tension steel plate using analysis and experiment. J Korea Acad-Ind Coop Soc 15:27–31. https://doi.org/10.5762/kais.2014.15.1.27

Kong YS, Cho HY (2018) Development of Sandwich structured seat Back frame using composite materials. Trans Korean Soc Mech Eng A 42:279–285. https://doi.org/10.3795/ksme-a.2018.42.3.279

Kong YS, Abdullah S, Omar MZ, Haris SM (2016) Topological and topographical optimization of automotive spring lower seat. Lat

Am J Solids Struct 13:1388–1405. https://doi.org/10.1590/1679-78252082

Li Q, Meng XX, Liu YB, Pang LF (2019) Risk assessment of floor water inrush using entropy weight and variation coefficient model. Geotech Geol Eng 37:1493–1501. https://doi.org/10.1007/s10706-018-0702-9

Lin C, Gao FL, Bai YC (2018) Multiobjective reliability-based design optimisation for front structure of an electric vehicle using hybrid metamodel accuracy improvement strategy-based probabilistic sufficiency factor method. Int J Crashworthiness 23:290–301. https://doi.org/10.1080/13588265.2017.1317466

Liu Z, Zhu C, Zhu P, Chen W (2018) Reliability-based design optimization of composite battery box based on modified particle swarm optimization algorithm. Compos Struct 204:239–255. https://doi.org/10.1016/j.compstruct.2018.07.053

Ma HF, Wang JX, Lu YN, Guo YW (2019) Lightweight design of turnover frame of bridge detection vehicle using topology and thickness optimization. Struct Multidiscip Optim 59:1007–1019. https://doi.org/10.1007/s00158-018-2113-1

Montoya MC, Costas M, Diaz J, Romera LE, Hernandez S (2015) A multi-objective reliability-based optimization of the crashworthiness of a metallic-GFRP impact absorber using hybrid approximations. Struct Multidiscip Optim 52:827–843. https://doi.org/10.1007/s00158-015-1255-7

Niresh J, Archana N, Raj GA (2019) Optimisation of linear passive suspension system using MOPSO and Design of Predictive Tool with artificial neural network. Stud inform. Control 28:105–110. https://doi.org/10.24846/v28i1y201911

Nguyen HT, Dawal SZM, Nukman Y, Aoyama H (2014) A hybrid approach for fuzzy multi-attribute decision making in machine tool selection with consideration of the interactions of attributes. Expert Syst Appl 41(6):3078–3090

Papaioannou G, Koulocheris D (2018) An approach for minimizing the number of objective functions in the optimization of vehicle suspension systems. J Sound Vib 435:149–169. https://doi.org/10.1016/j.jsv.2018.08.009

Pradhan MK (2013) Estimating the effect of process parameters on MRR, TWR and radial overcut of EDMed AISI D2 tool steel by RSM and GRA coupled with PCA. Int J Adv Manuf Technol 68:591–605. https://doi.org/10.1007/s00170-013-4780-9

Qader BS, Supeni EE, Ariffin MKA, Abu Talib AR (2019) RSM approach for modeling and optimization of designing parameters for inclined fins of solar air heater. Renew Energy 136:48–68. https://doi.org/10.1016/j.renene.2018.12.099

Qu LL, Zhou ZH, Zhang TZ, Zhang HN, Shi L (2019) An improved procedure to implement NSGA-III in coordinate waste management for urban agglomeration. Waste Manag Res 9. https://doi.org/10.1177/0734242x19865341

Safari H, Nahvi H, Esfahanian M (2018) Improving automotive crashworthiness using advanced high strength steels. Int J Crashworthiness 23:645–659. https://doi.org/10.1080/13588265.2017.1389624

Su ZY, Xu FX, Hua L, Chen H, Wu KY, Zhang S (2019) Design optimization of minivan MacPherson-strut suspension system based on weighting combination method and neighborhood cultivation genetic algorithm. Proc Inst Mech Eng Part D-J Automob Eng 233:650–660. https://doi.org/10.1177/0954407018789303

Sun GY, Zhang HL, Wang RY, Lv XJ, Li Q (2017) Multiobjective reliability-based optimization for crashworthy structures coupled with metal forming process. Struct Multidiscip Optim 56:1571–1587. https://doi.org/10.1007/s00158-017-1825-y

Wang YH (2015) Optimization analysis on car interior structure noise based on particle swarm optimization and RBF model. J Vibroeng 17:1499–1509

Wang C (2018) The improved elite multi-parent hybrid optimization algorithm based on bat algorithm to optimum design of automobile gearbox. J Discret Math Sci Cryptogr 21:513–517. https://doi.org/10.1080/09720529.2018.1449353

Wang P, Meng P, Zhai JY, Zhu ZQ (2013) A hybrid method using experiment design and grey relational analysis for multiple criteria decision making problems. Knowl-Based Syst 53:100–107

Wang ZJ, Dang SN, Xing Y, Li Q, Yan H (2015) Applying rank sum ratio (RSR) to the evaluation of feeding practices behaviors, and its associations with infant health risk in rural Lhasa. Tibet Int J Environ Res Public Health 12:15173–15181. https://doi.org/10.3390/ijerph121214976

Wang D, Jiang R, Lu W, Liu H (2016) Optimization of cab suspension parameters of self-dumping trucks using grey relational analysis. J Grey Syst 28(2)

Wang H, Bai QY, Hao XF, Hua L, Meng ZH (2018) Genetic algorithm-based optimization design method of the formula SAE racing car's rear wing. Proc Inst Mech Eng Part C-J Eng Mech Eng Sci 232:1255–1269. https://doi.org/10.1177/0954406217700181

Xiong F, Wang DF, Ma ZD, Chen SM, Lv TT, Lu F (2018a) Structure-material integrated multi-objective lightweight design of the front end structure of automobile body. Struct Multidiscip Optim 57:829–847. https://doi.org/10.1007/s00158-017-1778-1

Xiong F, Wang DF, Zhang SA, Cai KF, Wang S, Lu F (2018b) Lightweight optimization of the side structure of automobile body using combined grey relational and principal component analysis. Struct Multidiscip Optim 57:441–461. https://doi.org/10.1007/s00158-017-1749-6

Xiong F, Wang DF, Ma ZD, Lv TT, Ji LB (2019) Lightweight optimization of the front end structure of an automobile body using entropy-based grey relational analysis. Proc Inst Mech Eng Part D-J Automob Eng 233:917–934. https://doi.org/10.1177/0954407018755844

Yin S, Chen HY, Wu YB, Li YB, Xu J (2018) Introducing composite lattice core sandwich structure as an alternative proposal for engine hood. Compos Struct 201:131–140. https://doi.org/10.1016/j.compstruct.2018.06.038

Yuan Y, Xu H, Wang B (2014) An improved NSGA-III procedure for evolutionary many-objective optimization. In: Proceedings of the 2014 Annual Conference on Genetic and Evolutionary Computation. ACM, pp 661–668

Zeng F, Xie H, Liu QM, Li F, Tan W (2016) Design and optimization of a new composite bumper beam in high-speed frontal crashes. Struct Multidiscip Optim 53:115–122. https://doi.org/10.1007/s00158-015-1312-2

Zhang JY, Li ZY, Fang Q, Chen C (2019) Topological optimisation design of passenger car seat backrest frame based on multiple-loading conditions. Int J Crashworthiness 10. https://doi.org/10.1080/13588265.2019.1634355

Zhong J, Shi J, Shen J, Zhou G, Wang Z (2019) Engineering properties of engineered cementitious composite and multi-response optimization using PCA-based Taguchi method. Materials (Basel, Switzerland) 12. https://doi.org/10.3390/ma12152402

Zhu HJ, Yang J, Zhang YQ (2018) Modeling and optimization for pneumatically pitch-interconnected suspensions of a vehicle. J Sound Vib 432:290–309. https://doi.org/10.1016/j.jsv.2018.06.043

Zuo W, Yu J, Saitou K (2016) Stress sensitivity analysis andoptimization of automobile body frame consisting of rectangular tubes. Int J Automot Technol 17(5):843–851